1987-03

A technique for improving active network performance in a radiation environment without the use of hardened devices.

Lohr, David Michael

NAVAL POSTGRADUATE SCHOOL
Monterey, California

THESIS

A TECHNIQUE FOR IMPROVING ACTIVE NETWORK PERFORMANCE IN A RADIATION ENVIRONMENT WITHOUT THE USE OF HARDENED DEVICES

by

David Michael Lohr

March 1987

Thesis Advisor: S. Michael

URITY CLASSIFICATION OF THIS PAGE

REPORT DOCUMENTATION PAGE

REPORT SECURITY CLASSIFICATION JNCLASSIFIED	1b. RESTRICTIVE MARKINGS
SECURITY CLASSIFICATION AUTHORITY	3 DISTRIBUTION / AVAILABILITY OF REPORT Approved for public release; distribution is unlimited.
DECLASSIFICATION / DOWNGRADING SCHEDULE	
ERFORMING ORGANIZATION REPORT NUMBER(S)	5. MONITORING ORGANIZATION REPORT NUMBER(S)
NAME OF PERFORMING ORGANIZATION val Postgraduate School	6b OFFICE SYMBOL (If applicable) 62
7a. NAME OF MONITORING ORGANIZATION Naval Postgraduate School	
ADDRESS (City, State, and ZIP Code) nterey, California 93943-5000	7b. ADDRESS (City, State, and ZIP Code) Monterey, California 93943-5000
NAME OF FUNDING / SPONSORING ORGANIZATION	8b. OFFICE SYMBOL (If applicable)
9. PROCUREMENT INSTRUMENT IDENTIFICATION NUMBER	
ADDRESS (City, State, and ZIP Code)	10 SOURCE OF FUNDING NUMBERS

PROGRAM ELEMENT NO	PROJECT NO	TASK NO	WORK UNIT ACCESSION NO

TITLE (Include Security Classification)
TECHNIQUE FOR IMPROVING ACTIVE NETWORK PERFORMANCE IN A RADIATION VIRONMENT WITHOUT THE USE OF HARDENED DEVICES

PERSONAL AUTHOR(S)
hr, David Michael

TYPE OF REPORT	13b TIME COVERED	14 DATE OF REPORT (Year, Month, Day)	15 PAGE COUNT
ster's Thesis	FROM _____ TO _____	1987 March	153

SUPPLEMENTARY NOTATION

COSATI CODES			18 SUBJECT TERMS (Continue on reverse if necessary and identify by block number)
FIELD	GROUP	SUB-GROUP	Radiation Hardening; Composite Operational Amplifiers; Circuit Hardening

ABSTRACT (Continue on reverse if necessary and identify by block number)

This thesis examines and discusses the use of Composite Operational plifiers to reduce the sensitivity of active circuits to the degraded rformance of individual devices after exposure to radiation damage. mposite operational amplifiers, known to provide enhanced stability, creased sensitivity to circuit element variations and an extended eration frequency range, can be used to reduce circuit performance pendence on individual device parameter degradation under radiation thout the use of radiation hardened devices. If radiation hardened vices are used in the composite operational amplifiers, it should be ssible to achieve even higher levels of insensitivity to radiation. e composite operational amplifier is the only generalized method known provide radiation damage protection in this manner for active linear tworks.

DISTRIBUTION / AVAILABILITY OF ABSTRACT	21. ABSTRACT SECURITY CLASSIFICATION
X UNCLASSIFIED/UNLIMITED ☐ SAME AS RPT ☐ DTIC USERS	UNCLASSIFIED

NAME OF RESPONSIBLE INDIVIDUAL	22b TELEPHONE (Include Area Code)	22c. OFFICE SYMBOL
of Sherif Michael	(408)646-2252	62Mi

FORM 1473, 84 MAR — 83 APR edition may be used until exhausted. All other editions are obsolete — SECURITY CLASSIFICATION OF THIS PAGE

Approved for public release; distribution is unlimited

A Technique for Improving Active Network Performance in a Radiation Environment Without the Use of Hardened Devices

David Michael Lohr
Major, United States Marine Corps
B.S., United States Naval Academy, 1968

Submitted in partial fulfillment of the
requirements for the degree of

MASTER OF SCIENCE IN ELECTRICAL ENGINEERING

from the

NAVAL POSTGRADUATE SCHOOL
March 1987

ABSTRACT

This thesis examines and discusses the use of Composite Operational Amplifiers to reduce the sensitivity of active circuits to the degraded performance of individual devices after exposure to radiation damage. Composite operational amplifiers, known to provide enhanced stability, decreased sensitivity to circuit element variations and an extended operation frequency range, can be used to reduce circuit performance dependence on individual device parameter degradation under radiation without the use of radiation hardened devices. If radiation hardened devices are used in the composite operational amplifiers, it should be possible to achieve even higher levels of insensitivity to radiation. The composite operational amplifier is the only generalized method known to provide radiation damage protection in this manner for active linear networks.

TABLE OF CONTENTS

I. INTRODUCTION

The operational amplifier is easily one of the most widely used analog integrated circuits. In an effort to meet the ever increasing demands of the electrical engineering field, there have been many efforts to increase the capability of the amplifier.

One of the primary characteristics of the amplifier, that has been the object of extensive efforts for improvement, is the range of frequencies (bandwidth) that the amplifier can properly utilize when performing its basic functions. One answer to the problem of extending the amplifiers bandwidth is the composite amplifier [Ref. 1]. A composite amplifier consists of two or more individual amplifiers joined by a circuit that permits the entire group of amplifiers to perform as a single amplifier with improved characteristics.

The composite amplifier has many characteristics that are superior to those of a single amplifier. It is the object of this thesis to explore how one of those characteristics (increased bandwidth) can be of value in a high radiation environment. As a high level of radiation has a damaging effect on all amplifiers, it would be of great value to be able to reduce those negative effects through the replacement of single amplifiers with composite

amplifiers. The end result would be amplifiers and circuits that could function longer and better in the high radiation environments of space, nuclear reactors or closer to the explosion of nuclear weapons. That such a result can be realized through the superior bandwidth of composite amplifiers will be one of the areas explored by this thesis. Additionally, the characteristic of composite amplifiers to lose bandwidth due to damage at a slower rate than single amplifiers will also be evaluated.

Another area of performance that will be evaluated is the speed at which an amplifier operates (slew rate). As the composite amplifier assumes the slew rate of its component amplifiers, no improvement in performance is expected [Ref. 2]. The slew rate, however, should serve as a good indicator of the level of radiation damage sustained by the amplifier.

A final area of investigation will be the performance of single and composite amplifiers in a bandpass filter. The variation of the central frequency and the change in bandwidth due to radiation effects will also be evaluated in this thesis.

Chapter II discusses the effects of radiation on silicon devices, and the different techniques utilized to produce radiation hardened devices.

Chapter III traces the development of composite amplifiers. It concentrates on composite amplifiers that

have two component amplifiers. The theoretical basis for the performance of composite amplifiers is examined as well as the basic characteristics that are particularly relevant to this thesis.

Chapter IV introduces the characteristics of the Linear Accelerator (LINAC) at the Naval Postgraduate School. The method of utilizing the LINAC to evaluate the amplifiers at different radiation levels is also a part of this chapter. Additionally this chapter deals in detail with the procedures used to evaluate the characteristics of the single and composite amplifiers before and after being exposed to radiation.

Chapter V reports the results of the radiation testing of the amplifiers. Slew rate performance as well as bandwidth changes are discussed in detail. Additionally, the performance of the amplifiers as components of bandpass filters are detailed in this chapter.

Chapter VI is the final chapter and addresses the conclusions of the research conducted as a part of this thesis. Additionally, recommendations are made concerning future areas of research.

II. RADIATION

A. FORWARD

The semiconductor, integrated circuit is the heart of the electronic weapons and communication systems utilized by both military and civilian organizations. In many cases, it is desireable that these electronic systems work in hostile radiation environments that are both man made and natural. A hostile environment refers to space and nuclear reactors as well as nuclear weapons. To operate in these environments, the individual components are usually "hardened" to radiation.

It is the goal of this research to use unhardened components in specially designed circuits to minimize performance degradation in radiation environments. The object is to avoid the problems associated with hardening individual components by utilizing a circuit that provides radiation hardening while using "off the shelf" components. The radiation hardening is achieved by the special characteristics of the circuit which made the total circuit less sensitive to the degraded performance of the devices exposed to radiation.

B. RADIATION DAMAGE

"Radiation hardening" is the process that makes electronic components less vulnerable to damage or reduction in capability by radiation. Table 2.1 [Ref. 3] depicts the radiation sources that can cause radiation damage to electronic components.

The three major radiation sources consist of: (1) charged particles (ions, electrons, protons); (2) neutral particles (neutrons); and (3) photons (gamma rays, x-rays).

Charged particles primarily cause their radiation damage through the process of ionization. Charges particles and photons cause equal amounts of ionization damage to semiconductor material when applied in equal doses (Rads(Si)). [Ref. 4] The dose indicates the amount of energy, expressed in rads (100 ergs/gram), that is deposited in a material. The dose rate has been found to be an important factor when considering the effects of radiation on semiconductors [Refs. 5, 6, 7]. When the same total dose is applied at different dose rates, different levels of radiation damage occur in the device. Ionizing radiation causes induced trapped charge and interface states at the silicon-insulator boundary.

Neutrons primarily cause damage through the displacement of lattice atoms in the crystal structure of the semiconductor material.

TABLE 2.1 RADIATION SOURCES

Sources	Radiation	Output
Natural Radioactive Material		
Uranium, Radium, Radon	alpha, beta, gamma	2.3 rads/hr
Irradiated Materials		
Cobalt-60, Sodium, Iodine	alpha, beta, gamma	to 10^7 rads/hr
Fission Fragments		
Strontium, Cesium	alpha, beta, gamma	10^9 rads/hr and up
From Space		
Cosmic radiation	nuclei	2 particles/cm²-sec (kinetic energies of 1 to 10 BeV)
Solar Flares	protons	1000 rads/hr
Van Allen Belts	electrons	10 rads/hr
Reactors	gamma	10^7 rads/sec
	neutron	$\approx 10^{15}$ neutrons/cm²-s
Fission/Fusion Weapons (Percentage of weapon output)	alpha, beta	27.5%
	gamma	0.5%
	neutrons	2.0%
	x-rays	70.0%

To offset the effects of these three major sources of radiation, semiconductor devices are hardened through a combination of special processing and careful control of the geometry of the devices structure. [Ref. 8] Special processing and geometry require more manufacturing steps and hence cost more money than the processes for unhardened devices. Additionally, the geometric adjustments required for hardening the semiconductor devices reduces the packing density on the chip; further increasing costs. Instead of pursuing a manufacturing technique that will both reduce price and increase chip density; it is the object of this thesis to demonstrate a technique whereby the desired hardening is achieved through the arrangement of special circuits using normal nonhardened components.

The specific method of radiation damage utilized during the course of this research was bombardment of the semiconductor devices with high energy electrons. The following is a description of the types of radiation damage produced by high energy electrons and the method of measurement of the amount of damage.

Inelastic Coulomb Scattering is the primary means by which electrons lose energy as they strike a target. The energy is lost through both ionization and Bremsstrahlung. [Ref. 9] Stopping power is the energy lost by a particle per unit length of path through a material [Ref. 10]. The

amount of material required to stop the bombarding particles is a measure of the stopping power of the material. The stopping power used in this thesis is detailed in Chapter IV.

The ionization process involves the inelastic collision of the high energy incident electron with electrons associated with atoms (atomic electrons). The collisions excite or free the atomic electrons (Figure 2.1) resulting in a change in energy for the beam electron.

The Beamsstrahlung process results from the common phenomenon of an accelerated charge particle radiating energy (photons). When the beam electrons have their direction of travel changed by inelastic Coulomb collisions with the nucleus or atomic electrons, they will radiate as depicted in Figure 2.2. The radiation represents an energy decrease for the beam electrons and is called Bremsstrahlung radiation. [Ref. 11]

Elastic collisions between the beam electron and the nucleus of an atom can also reduce the energy of the beam electron. The kinetic energy imparted to the nucleus of the atom can cause the atom to transfer energy to the rest of the surrounding atoms; heating the crystal lattice. The collision can also eject the atom from its place in the structure; given enough energy other atoms will in turn be displaced by the first atom in a cascading fashion, producing displacement defects (Frenkel defects). [Ref. 12] Due to

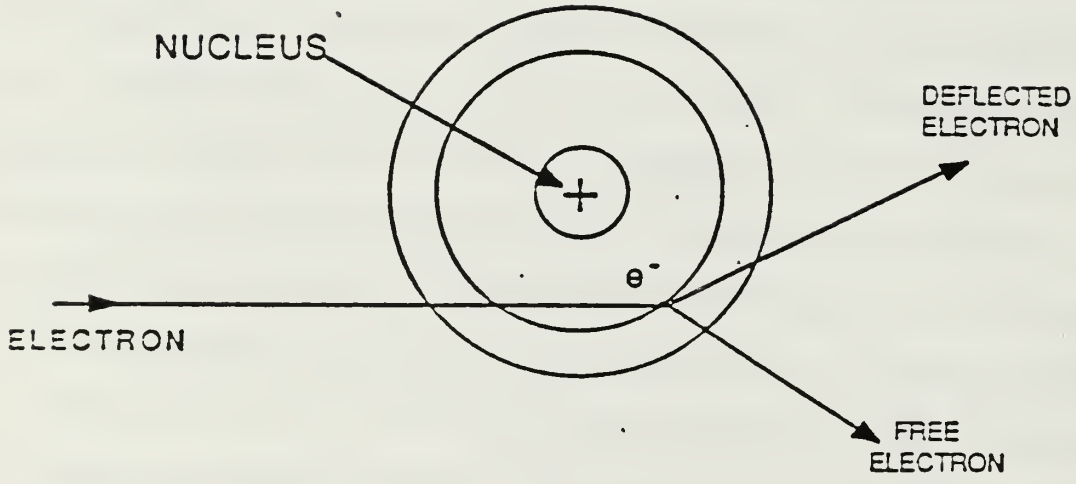

Figure 2.1 Freeing of an Electron by Inelastic Collision of a Beam Electron with a Target, Atomic Electron

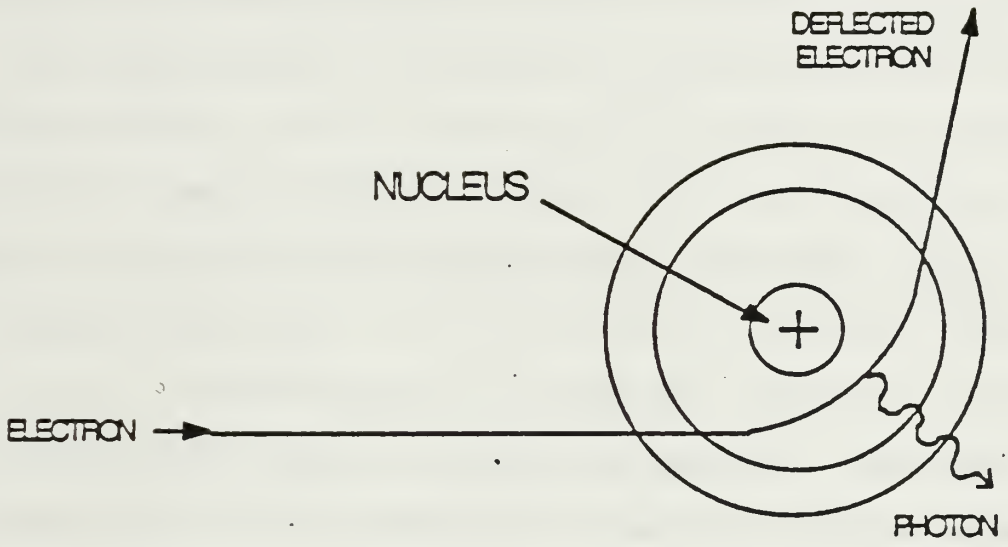

Figure 2.2 Creation of a Photon by Bremsstrahlung

the relative masses of the electron to the nucleus, very little energy is transferred in this manner.

The two methods of measuring damage caused by radiation are range and dose. Range is the path length an electron travels while being brought to rest in a material and has units of grams per square centimeter [Ref. 9]. As the electrons are assumed to lose energy continuously, the range can be divided by the density of the material to determine the distance an electron is most likely to travel. For the 30 MEV electrons used in the NPS linear accelerator, the range in silicon is 13.83 g/cm2 with the most probable distance traveled 5.94 cm,[Ref. 13] Range was not used as a method of damage measurement in this thesis.

The dose represents an amount of energy deposited in the material and is the measure of damage used in this thesis. Dose is expressed in rads (100 ergs/gram) if one square centimeter of surface material is assumed and the surface material specified. The specific doses used in this thesis are explained fully in Chapter IV. Dose was calculated in this thesis from the voltage deposited on a capacitor by the electron beam. The specific details of dose measurement are explained in Chapter IV.

C. EFFECT OF RADIATION ON ACTIVE DEVICES

As stated earlier in the previous chapter, our concern in this research is to improve active circuit performances

employing operational amplifiers exposed to radiation environments. In this section, a brief introduction to some of the main device parameters affected by radiation is presented. In the first case of bipolar amplifiers the transistor parameter g_m is chosen. The transistor transconductance (g_m) affects a variety of amplifier characteristics [Ref. 14]:

1) Open loop gain
2) Slew rate
3) Gain bandwidth product (GBWP)
4) Neutron induced offset current and voltage drift
5) Gamma threshold
6) Output voltage swing

The GBWP and slew rate of operational amplifiers are of great importance in this research. These two characteristics, as well as all the others, are affected by radiation and the extent to which they are affected is detailed in the following chapters of this thesis.

The effects of ionizing radiation on the gain of bipolar junction transistors (BJT) can be best described by examing the changes in the components of the base current as a function of radiation.

The base current components are composed of surface related electron-hole recombination-generation type terms and diffusion ("bulk") related terms.

The recombination-generation terms at the surface are defined for depletion layers (DL) near the surface of the semiconductor. These terms describe the contributions to the base current from a field-induced depletion region formed in the base near the surface (I_{FIDL}), and the recombination-generation of electron-hole pairs at the surface (I_{SO}). Two other possible surface terms are defined when the new surface depletion layer is complete and exist only after I_{SO} has peaked. The new terms are I_{RBDL} (due to electron recombination (RB) in the new depletion layer (DL)), and $I_{D'DL}$ (due to hole recombinations (D') in the new depletion layer (DL)).

The effects of increasing ionizing radiation (high dose levels) on the I_{FIDL} to increase I_{FIDL}. The increase in I_{FIDL} is a result of the change in recombination rate near the surface. [Ref. 15]

At higher dose rates, another effect is expected; the high dose levels cause the surface state density to become dominant. The surface state density dominance forces the surface potential to a point where I_{SO} peaks.

The bulk surface dependent diffusion currents are affected by the increased ionization due to high dose rates. Large surface potentials can induce a full depletion layer at the surface. The effects of ionization radiation on the surface potential (ϕ_S) profile can be seen in Figure 2.3. The profile represents the surface potential as seen by the

charge carriers in the semiconductor near the surface. The surface potential is modeled from the edge of the emitter-base depletion layer versus distance from the metallurgical junction.

Another view of the depletion layer created at the surface is that this depletion layer is an extension of the emitter-base junction depletion layer. The extension of the depletion layer causes the additional base current components of I_{RBDL} and $I_{D'DL}$. Of these two terms, only the $I_{D'DL}$ term responds to radiation and that response is small in comparison to I_{SO} especially at a low V_{BE}.[Ref. 16]

The final result of the increased ionization due to high dose levels is an increase in the base current as its components are increased by the radiation. The two important parameters that determine this change in base current are the surface potential, and the interface (surface) state density. The interface density is assumed to build up with the same field dependence as the trapped charge.[Ref. 16] The resulting field-dependent surface potential distribution (Figure 2.3) was used in determining the added base current resulting from ionizing radiation for a BJT (an ungated 2N222 transistor in this case). By using a simple approach to add the contributions of the components of the base current, an expected change in base current can be developed (Figure 2.4).

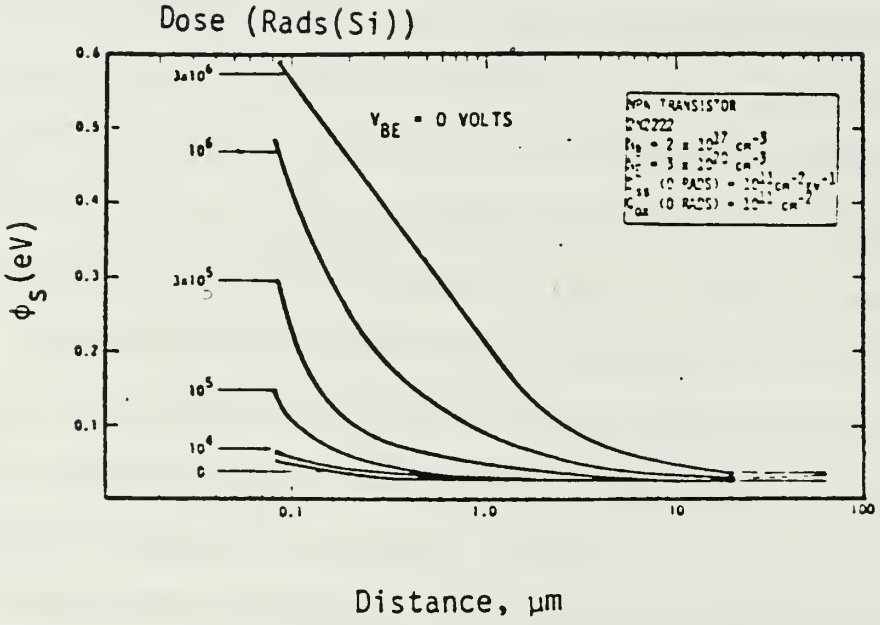

Figure 2.3 Surface Potential Profile

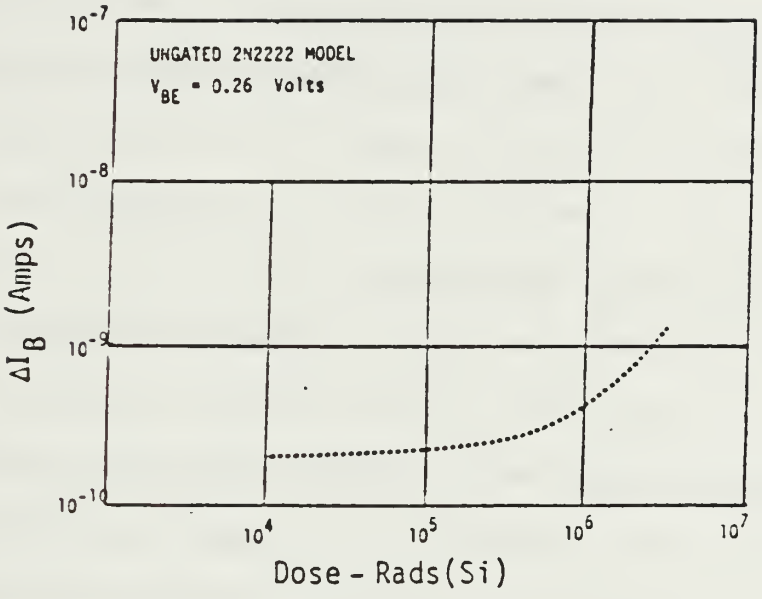

Figure 2.4 Expected Change in Base Current

The expected increase in the base current (I_B) will result in a decrease in the transconductance (g_m) and the current gain (β) of the BJT transistors as they have an inverse relationship. The gain $\beta = I_C/I_B$ and $g_m = \beta/r_\pi$, where I_C is the collector current the r_π is the small signal base-emitter resistance. The decrease in gain of the transistor will in turn affect the overall amplifier voltage gain. The resulting loss in gain means the gain-bandwidth product is reduced; therefore when the gain of a device is held constant, the expected effect of radiation is to reduce the 3 dB frequency of the device.

The physical effect of the ionizing radiation on the JFET devices is very much the same as the junction boundary effects of the BJT devices. The most important effect of the radiation is the increase in the depletion region of the JFET devices. Increasing the depletion region of the JFET devices has the effect of reducing the channel width, thus the radiation reduces the potential flow of channel current and consequently reduces the potential gain that the JFET amplifiers can achieve. The reduction in gain also appears as a loss in GBWP, and the 3 dB frequency will thus be smaller for a constant gain.

D. RADIATION HARDENED DEVICES

The normal means of hardening a circuit is to harden its components, vice the techniques introduced in this thesis.

The experiments in this thesis relied on the design of the circuits to produce hardening vice special processing of the individual components.

The technology choices that produce radiation hardness are the basic factors in present efforts to harden circuits to radiation. In silicon technology the choice of active devices is limited to the following general types:

1) Bipolar junction transistors (BJT)
   a) NPN (NBJT)
   b) PNP (PBJT)
2) Junction field effect transistors (JFET)
   a) N-channel (JFET)
   b) P-channel (PJFET)
3) Metal-oxide-silicon field effect transistors (MOSFET)
   a) N-channel (NMOS)
   b) P-channel (PMOS) [Ref. 14]

Considering the additional factors of structure (vertical or lateral), isolation (dielectric or junction), dopants (diffused or implanted), etc.; there are a very large number of alternative ways of combining these devices.

Some of the factors that reduce the possible combinations of these devices are:

1) Noncomplementary combinations are infeasible (i.e., single active device types or NXXX/NXXX or PXXX/PXXX).
2) Some structures have totally inadequate radiation hardness (i.e., lateral and substate BJT devices.

3) Assuming bulk device technology, only dielectric oxide isolated structures are suitable to withstand transient radiation.

4) Certain active device combinations are process incompatible and infeasible in monolithic technology (i.e., NPN+PNP+NJFET+PJFET).

5) Performance and producibility factors eliminate other devices,[Ref. 14]

The monolithic implementation is generally preferable in the production of radiation hardened devices,[Ref. 14] The following is a list of "viable" active devices.

1) NBJT (vertical) Figure 2.5

2) PBJT (vertical) Figure 2.5

3) NJFET (diffused) Figure 2.6

4) PJFET (ion implanted) Figure 2.7

5) NMOS (depletion) Figure 2.8

6) PMOS (enhancement Figure 2.9 [Ref. 14]

"Viable" is a term that encompases many factors; radiation hardness, electrical characteristics, and producibility. The referenced figures illustrate the topology and vertical structure of these devices. It is assumed that a dielectric isolation structure will be employed. Active device processing is essentially the same for dielectric or junction isolation processes.

The monolithic process that is used to produce the radiation hardened devices is complex and its many aspects must be carefully considered before each application. The compatibility of the diffusion operations is the major

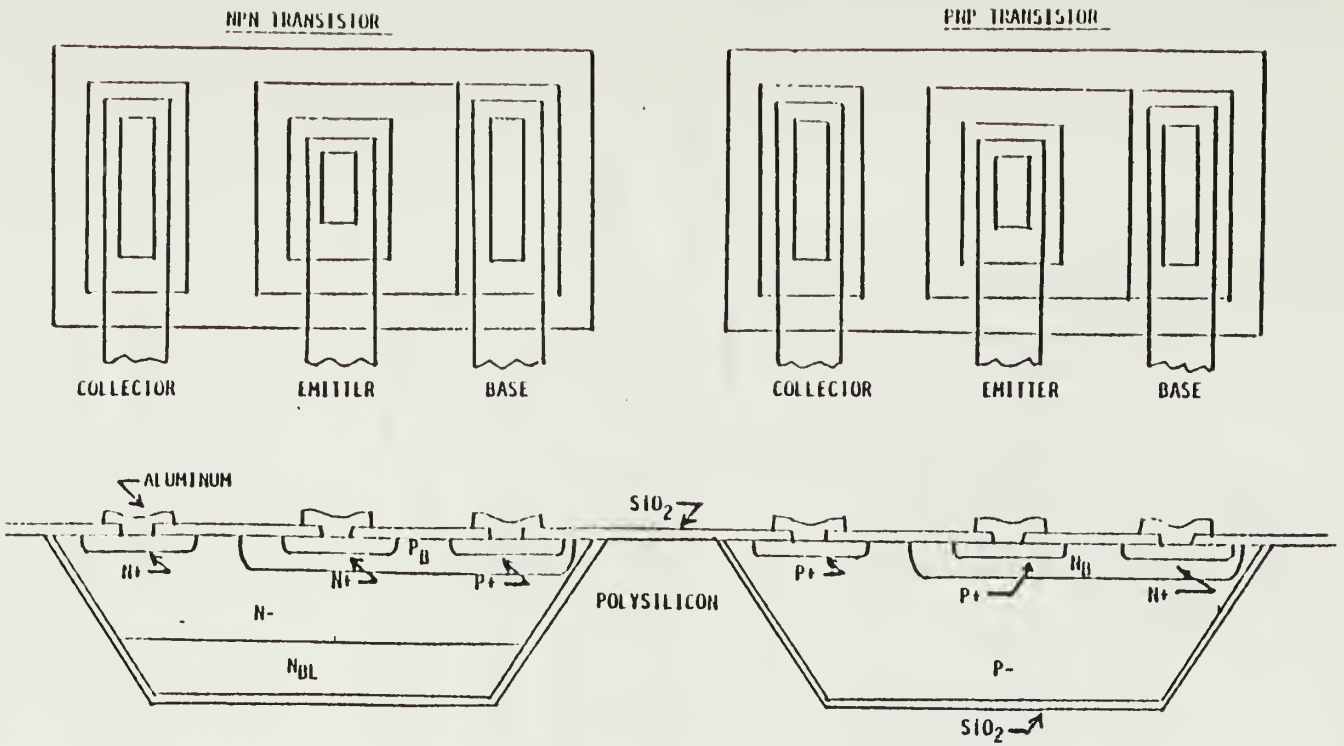

Figure 2.5 NPN and PNP Transistors

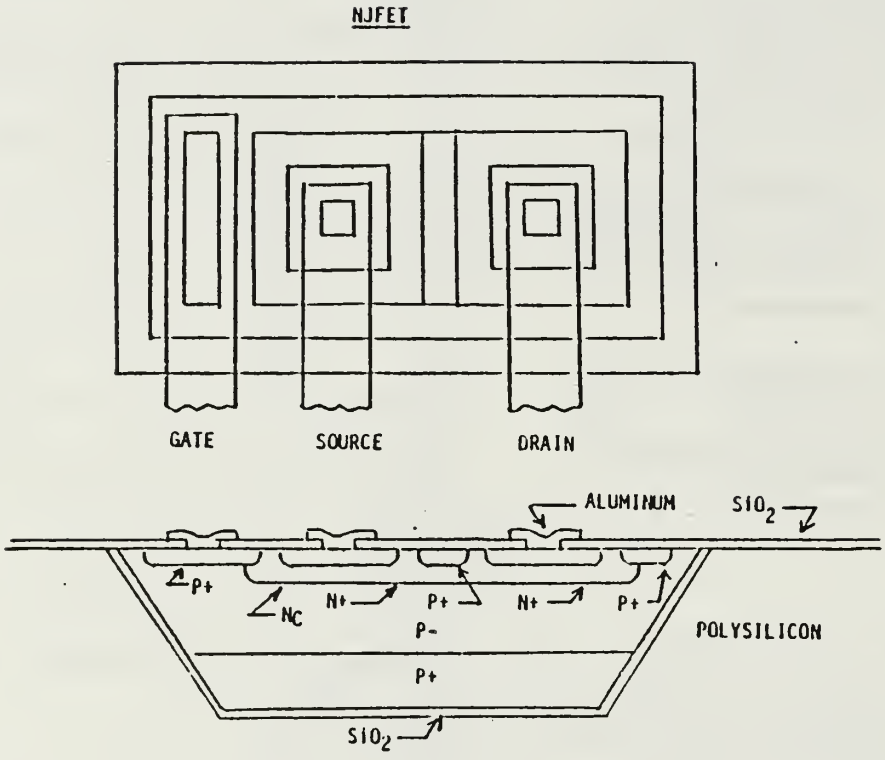

Figure 2.6 NJFET Transistor

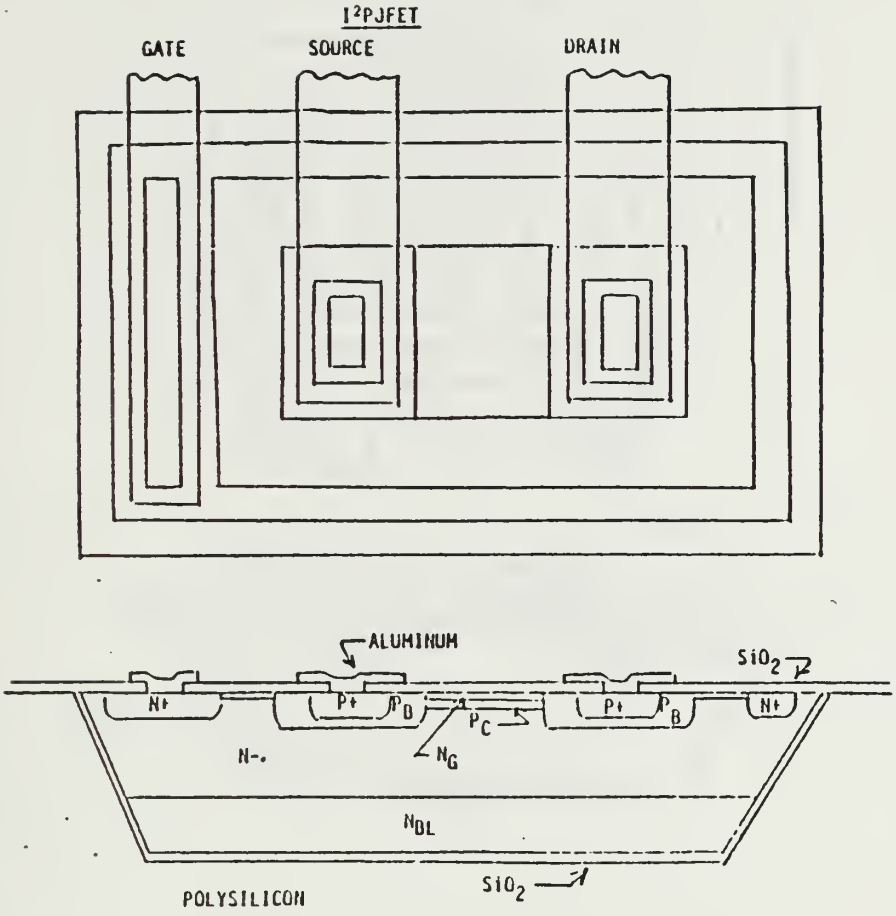

Figure 2.7 PJFET Transistor

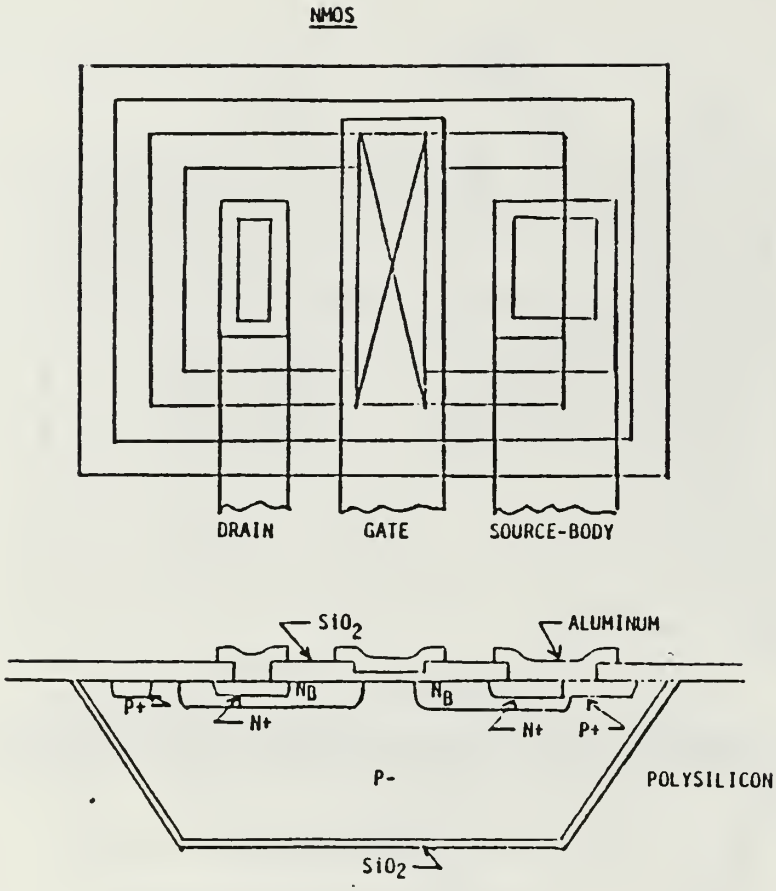

Figure 2.8 NMOS Transistor

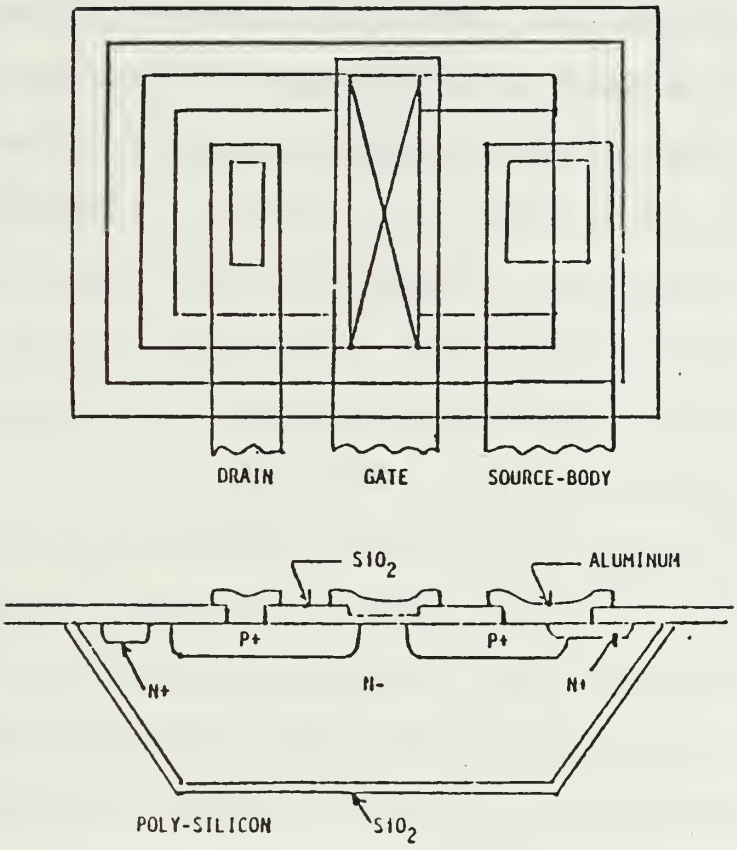

Figure 2.9 PMOS Transistor

consideration in the production of the active devices. Diffusion process is interpreted to include conventional diffusion, oxidation and ion implantation. The primary difficulty encountered with diffusion is time/temperature factors. As the various structures of the devices are fabricated through a sequence of diffusion operations, each diffusion operation has a time/temperature impact on the previous diffusion operations. Consequently, each succeeding diffusion operation must be time/temperature compatible with previous diffusion operations.[Ref. 14]

The compatibility of diffusion operations is complicated by the fact that different diffusion species (boron, phosphorous, arsenic, etc.) have different diffusion coefficients and different temperature dependencies. Similar considerations apply to critical oxidation operations and to ion implanted structures. Additionally, integrated circuits of the type desired typically involve several hundred operations during the course of construction. Each step of the process requires rigid control or the result will be a very small percentage of acceptable devices.[Ref. 14]

It is the object of this thesis to suggest an alternative to the special process of producing radiation hardened devices. Instead of complicating the already complex process of device production, it is suggested that nonhardened devices can be employed in specially designed circuits to produce radiation hardening. This technique will incorporate

some special designs that proved to possess excellent active and passive sensitivities, thus reducing the circuit performance dependence on individual device parameter degradation under radiation. These designs are referred to as Composite Operational Amplifiers and are presented in the following chapter.

III. COMPOSITE AMPLIFIERS

Linear active circuits (positive, negative and differential finite gain amplifiers, integrators and active filters) are mainly realized using operational amplifiers (OA's) as the active elements. Linear active circuits have limited operating frequencies due to the frequency dependent gains of their active elements. Operating frequencies are here defined as those frequencies at which linear active circuits will operate without deviation from their theoretical design values by more than a predetermined acceptable range.

In practical applications, the passive components (resistors, capacitors, etc.) have a limiting influence on the operating frequencies at a much higher range of frequencies than the limitations imposed by the OA's. Consequently, the actual input to output relationship $T_a(s)$ of the active circuit will differ from the ideal mathematical input-output relationship $T_i(s)$; even if all the passive components in the circuit are ideal. Variations in frequency, temperature and power supply will cause OA parameter variations which will cause corresponding changes in $T_a(s)$; the less the dependence of $T_a(s)$ on the OA parameters, the smaller the variations in $T_a(s)$.

Composite Operational Amplifiers (CNOA) (N indicates the number of component amplifiers) are a new approach for extending the useful Bandwidth (BW) of linear active circuits. It can be easily shown that by replacing each OA in any circuit design with a CNOA, without changing the comparison network, serves to extend the BW of this design. The CNOA is constructed of N regular OA's. The resulting CNOA has 3 terminals; an inverting input, a non-inverting input, and an output. The CNOA's allow both amplitude and phase active compensation using resistor ratios as the controlling parameters. The CNOA has the same versatility as an OA. The use of CNOA's in popular active realizations will greatly extend the useful range of operating frequencies over realizations that use a similar number of single OA's (N).

In this chapter, the procedure for generating C2OA's using nullator, norator pairing will be presented [Refs. 17, 18, 19], these are theoretical networks shown in Figure 3.1. The nullator is a one port which neither sustains a voltage nor passes a current (i.e., V=I=0). On the other hand, the norator is a one port which will sustain an arbitrary voltage and pass an arbitrary current (the current and voltage are independent of each other). A set of useful performance criteria for determining which C2OA's to retain will be introduced; only four C2OA's meet these criteria and are retained. The applications of the $C2OA_i$'s (i=1 to 4)

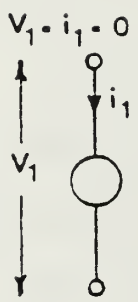

The Nullator

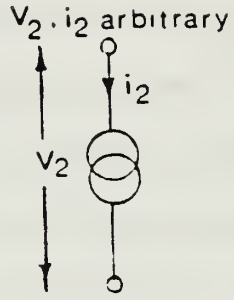

The Norator

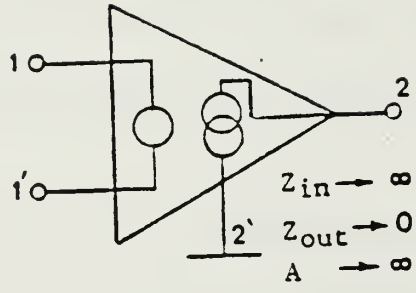

The OA (VCVS) Nullor Representation

Figure 3.1 The Singular Elements Representation of the OA

in negative, positive and differential finite gain amplification will also be presented. The performance improvement of the resulting active circuits are examined and found to compare favorably with the best existing realizations employing a similar number of OA's.

A. GENERATIONS OF THE C2OA'S

An operational amplifier (Figure 3.2) is a Voltage Controlled Voltage Source (VCVS). In the ideal case, the input impedance Z_{in} approaches infinity, the output impedance Z_{out} approaches zero and the open loop gain approaches infinity. The corresponding idealized model (Figure 3.1) is composed of two singular elements; the nullator and norator. [Refs. 17, 18, 19] The ideal OA is replaced by a nullor having the following characteristics:

$$\begin{bmatrix} V_1 \\ I_1 \end{bmatrix} = \begin{bmatrix} 0 & 0 \\ 0 & 0 \end{bmatrix} \cdot \begin{bmatrix} V_2 \\ -I_2 \end{bmatrix} \qquad (1)$$

which is called the nullor chain transmission matrix of an ideal OA. In any physical circuit that contains N OA's, if each OA is replaced by a nullor, we obtain a nullor equivalent network. The nullors then can be split into nullators and norators to yield a nullator-norator equivalent network.

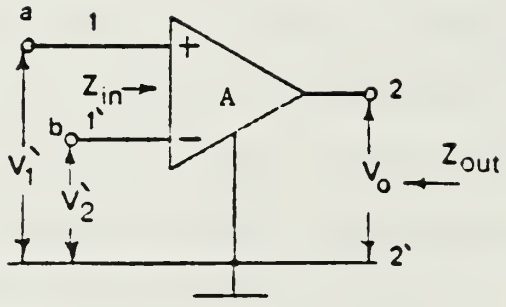

Figure 3.2 Circuit Symbol for the Operational Amplifier (OA)

In reverse, a nullator-norator equivalent network containing n nullators and n norators yields n! nullor equivalent networks, since nollators and norators can be paired into nullors in an arbitrary manner. For example, a nullator-norator equivalent network containing two nullators and two norators yields two nullor equivalent networks. Nullator X can be paired with norator X or Y, and nullator Y can be paired with norator Y or X, as shown in Figure 3.3.

Although the nullator (or norator) is not admissible as an idealization of a physical network, the nullor, like an infinite-gain controlled source, is admissible. The equivalence established is valid whether $A \to \infty$ or $A \to -\infty$ and so in practice, a nullor can be replaced by a high-gain differential controlled source in two ways as shown in Figure 3.4. Consequently, the noninverting-input terminal of the controlled source can be connected to a node K, and the inverting-input terminal to a node L (Figure 3.4b) or vice-versa (Figure 3.4c). Thus a nullor equivalent network containing two nullors corresponds to four physical networks, since either high-gain controlled source can be connected in two ways. In general, a nullor equivalent network containing n nullors corresponds to 2^n physical networks. Each of these n! nullor networks yields a physical realization which has a different dependence on the non-ideal active elements.

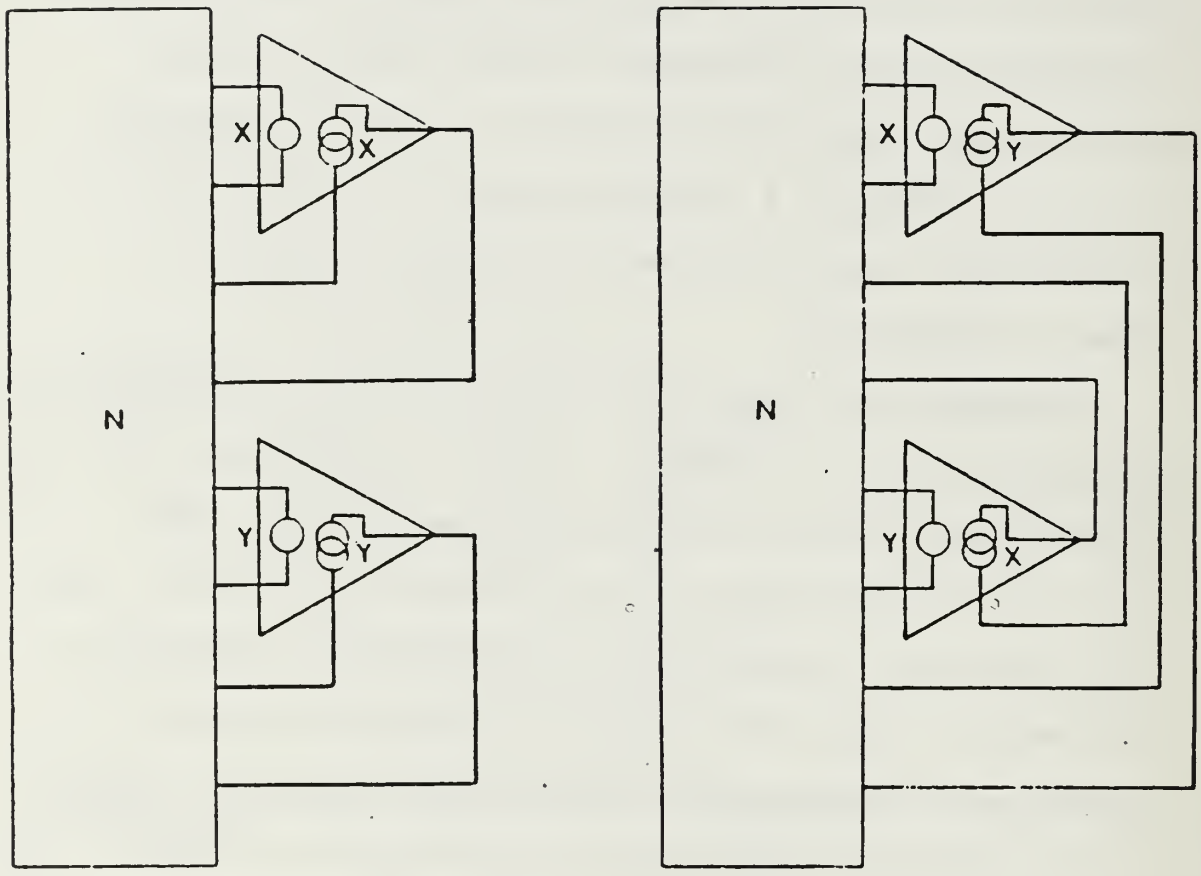

Figure 3.3 Two Alternative Nullor Equivalent Networks Obtained From a Single Nullator-Norator Equivalent Network

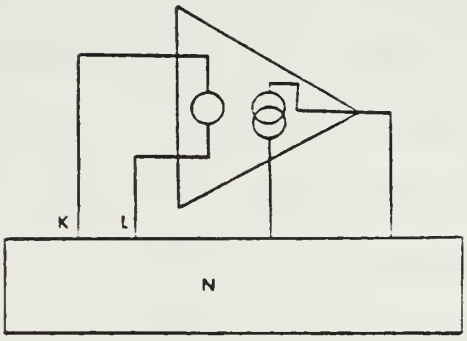

Figure 3.4.a Circuit Containing One Nullor

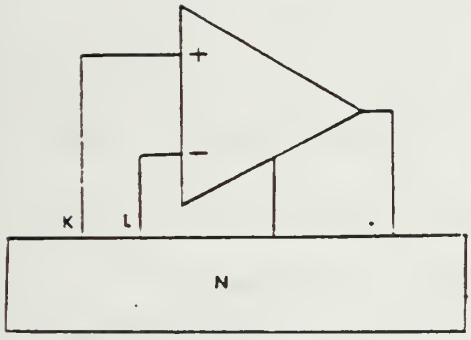

Figure 3.4.b

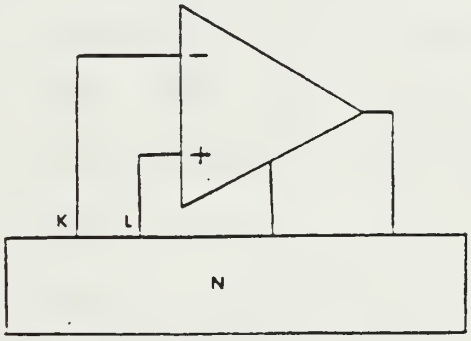

Figure 3.4.c

Figure 3.4.b,c Two Alternative Physical Circuits

Figure 3.4 Replacement of Nullors by Physical Networks

After this brief explanation, the procedure to generate the C20A's is described as follows. In the first step, a redundant amplifier of finite gain $\pm$ H is combined with a single OA, such that the chain matrix of the resulting two amplifier network, assuming ideal amplifiers, corresponds to that of a nullor, as given by equation (1). In other words, although each network contains 2 VCVS's, the overall two-port network realizes one VCVS. Six topologies are obtainable from each of the four networks shown in Figures 3.5a and 3.5b. Two topologies are obtained, one for +H and the other for -H, Figure 3.5e, f, at each position of the three way switch, leading to six topologies per network. It is easy to show that 17 out of the 24 topologies realize true nullors, i.e., none of the network elements or signals are required to assume certain values. Eight possible OA realizations can be obtained from each of these seventeen topologies (nullor) networks. This results in 136 Composite Operational Amplifiers (C20A's), each constructed using two singla OA's. The resulting C20A's, are examined according to the following performance criterion [Ref. 1]:

1) Let $A_a(s)$ and $A_b(s)$ be the non-inverting and inverting open loop gains of each of the 136 C20A's examined. The denominator polynomial coefficients of $A_a(s)$ and $A_b(s)$ should have no change in sign; this satisfies the necessary (but not sufficient) conditions for stability. Also, none of the numerator or denominator coefficients of $A_a(s)$ and $A_b(s)$ should be realized through differences. This eliminates the need for single OA's of matched GBWP's and results in low sensitivity of the C20A with respect to its components.

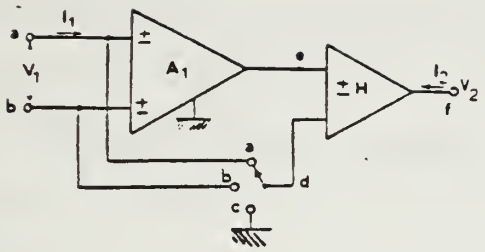

Figure 3.5.a

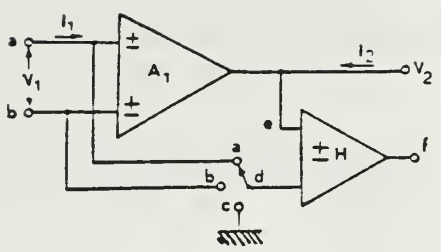

Figure 3.5.b

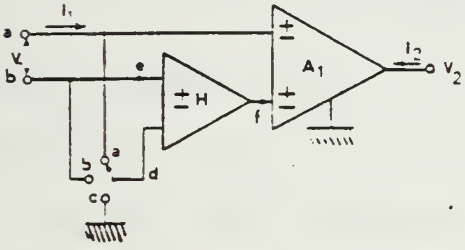

Figure 3.5.c

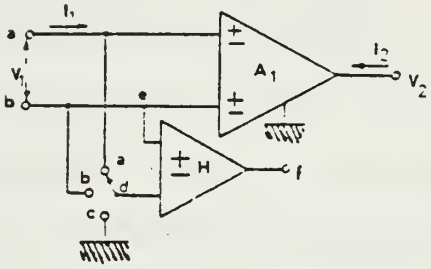

Figure 3.5.d

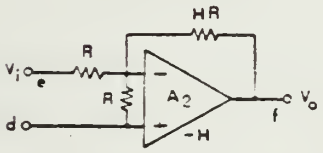

Figure 3.5.e

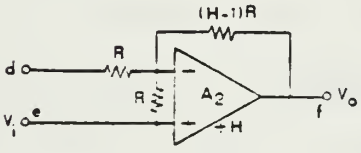

Figure 3.5.f

Figure 3.5.a-d The Four Different Networks for Generating the Composite Operational Amplifiers Using Two Single OA's (C2OA's)

Figure 3.5.e,f The +H and -H Finite Gain Amplifier Realizations Used in Figures 3.5.a to 3.5.d

2) The external three terminal performance of the $C20A_i$ should resemble, as closely as possible, from the versatility point of view, that of the single OA.

3) To minimize phase shift, no right half S plane (RHS) zeros should be allowed in the C20A's closed loop gains. The RHS zeros can be due to the single OA pole.

4) The resulting input-output relationship $T_a(s)$ in the applications considered should have extended frequency operation with minimum gain and phase deviation from the ideal $T_i(s)$. The improvement should be enough to justify the increased number of OA's.

Four C20A's referred to as C20A-1, C20A-2, C20A-3, and C20A-4 out of the 136 examined, are found to have acceptable performance according to the above criterion [Ref. 20].

It is interesting to note that by applying the nullator-norator concept to the transistors in a Darlington pair, C20A-3 can be obtained.[Ref. 21] Thus, C20A-3 with a compensation resistor ratio (α) of zero, can be considered as a special case of the Darlington network, since the norators are both ac grounded in the Darlington pair nullator network to be able to convert it into an OA realization.

The open loop gain of the single OA's, used in constructing the C20A's, assuming a single pole model, can be expressed as:

$$A_i = A_{oi}w_{Li}/(w_{Li} + s) = w_i/(s + w_{Li}) \qquad (2)$$

$i = 1$ or 2

where A_{oi}, w_{Li} and w_i are the dc open loop gain, the 3-dB Bandwidth, and the GBWP of the i^{th} single OA respectively.

It can be easily shown that the open loop input-output relationships of C20A-1 to C20A-4 are given by:

$$V_{oi} = V_a A_{ai}(s) - V_b A_{bi}(s) \qquad (i = 1 \text{ to } 4)$$

where for C20A-1:

$$V_{o1} = (V_a A_2(1 + A_1)(1 + \alpha) - V_b A_1 A_2(1 + \alpha))/(A_1 + (1+\alpha)) \qquad (3)$$

for C20A-2:

$$V_{o2} = (V_a - V_b)(A_1 A_2(1 + \alpha))/(A_2 + (1+\alpha)) \qquad (4)$$

for C20A-3:

$$V_{o3} = (V_a A_1 A_2 - V_b A_2(1 + A_1))/(1+ \alpha) \qquad (5)$$

and for C20A-4:

$$V_{o4} = (V_a A_2(A_1 + \alpha) - V_b A_2(A_1 + (1 + \alpha)))/(1+\alpha) \qquad (6)$$

where α is a resistor ratio [Ref. 20].

Assuming identical OA's, i.e.:

$$A_{o1} = A_{o2} = A_o \text{ and } w_1 = w_2 = w_i$$

it is interesting to examine the open loop gains given by equation (3) to equation (6) in the single ended inverting application, i.e., $V_a = 0$. For C20A-1 and C20A-2 the dc gain A is given by:

$$A_{oC1} = A_o(1 + \alpha)/1 + (1 + \alpha)/A_o \qquad (7.a)$$

$$\simeq A_o(1 + \alpha) \text{ for } (1 + \alpha) << A_o$$

From (7.a), the composite amplifier has a single pole roll off from w_i/A_o to $w_i/(1 + \alpha)$ where the second pole occurs. As α increases, the dc gain increases while the second pole frequency decreases. Also, from equation (4) and equation (5), each of C20A-3 and C20A-4 has a dc gain given by:

$$A_{oC2} = A_o 2/(1 + \alpha) \qquad (7.b)$$

A_{oC2} has double poles (12 dB/octave) at w_i/A_o, and as α increases the dc gain decreases without affecting the second pole location.

Only C20A-2 has identical expressions for the positive and negative open loop gains A_a and A_b. Thus Common Mode Rejection Ratio (CMRR) problems should not be encountered using C20A-2 even for relatively large common mode signal applications. From equation (3), equation (5) and equation (6), the CMRR of C20A-1 and C20A-3 is $(A_{o1} + 1/2)$, while that of C20A-4 is $(A_{o1} + \alpha + 1/2)$. For single ended applications (small common mode signal), no problem should be encountered using C20A-1, C20A-3 and C20A-4.

It is important and easy to show that the voltage swing at the first OA(A_1) output, which is an internal node, in each of C20A-1 to C20A-4, is always less than the output voltage V_o. Hence the dynamic range is determined by the voltage swing of the output voltage V_o. Thus no dynamic range reduction of V_o or harmonic distortion problems should arise.

B. REALIZATION OF POSITIVE, NEGATIVE, AND DIFFERENTIAL FINITE GAIN AMPLIFIERS USING THE PROPOSED C20A'S

The application of the four proposed C20A's in positive and negative finite gain amplification is given in Table 3.1. Also, for the sake of illustration, the use of a C20A-2 as a differential finite gain amplifier, Figure 3.6, can be shown to have the input-output relationship given by:

$$V_o = T_{i1}(1/(1 + s/w_pQ_p + s^2/w_p^2))V_1 + T_{i2}(1/(1 + s/w_pQ_p + s^2/w_p^2))V \quad (8)$$

TABLE 3.1 NEGATIVE AND POSITIVE FINITE GAIN TRANSFER FUNCTIONS USING THE C20A'S

C20A	Negative Finite Gain Trans. Function (T_a)	Positive Finite Gain Trans. Function (T_a)	ω_p	Q_p
C20A-1	$T_f \dfrac{1}{1 + (S/\omega_p Q_p) + (S^2/\omega_p^2)}$	$T_f \dfrac{(1+S/\omega_1)}{1 + (S/\omega_p Q_p) + (S^2/\omega_p^2)}$	$\sqrt{\dfrac{\omega_1\omega_2}{1+k}}$	$\dfrac{(1+\alpha)}{\sqrt{1+k}}\sqrt{\dfrac{\omega_2}{\omega_1}}$
C20A-2	$T_f \dfrac{1}{1 + (S/\omega_p Q_p) + (S^2/\omega_p^2)}$	$T_f \dfrac{1}{1 + (S/\omega_p Q_p) + (S^2/\omega_p^2)}$	$\sqrt{\dfrac{\omega_1\omega_2}{1+k}}$	$\dfrac{(1+\alpha)}{\sqrt{1+k}}\sqrt{\dfrac{\omega_1}{\omega_2}}$
C20A-3 *	$T_f \dfrac{(1+S/\omega_1)}{1 + (S/\omega_p Q_p) + (S^2/\omega_p^2)}$	$T_f \dfrac{1}{1 + (S/\omega_p Q_p) + (S^2/\omega_p^2)}$	$\sqrt{\dfrac{\omega_1\omega_2}{(1+k)(1+\alpha)}}$	$\sqrt{\dfrac{(1+k)(1+\alpha).\omega_1}{\omega_2}}$
C20A-4	$T_f \dfrac{[1+(1+\alpha)S/\omega_1]}{1 + (S/\omega_p Q_p) + (S^2/\omega_p^2)}$	$T_f \dfrac{(1+\alpha S/\omega_1)}{1 + (S/\omega_p Q_p) + (S^2/\omega_p^2)}$	$\sqrt{\dfrac{\omega_1\omega_2}{(1+k)(1+\alpha)}}$	$\sqrt{\dfrac{(1+k)}{(1+\alpha)}\cdot\dfrac{\omega_1}{\omega_2}}$
	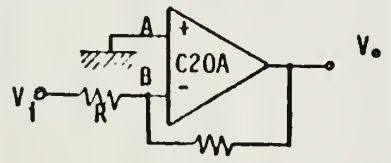	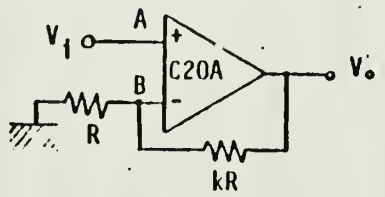		
	$\dfrac{V_o}{V_i} = -k = T_f$	$\dfrac{V_o}{V_i} = (1+k) = T_f$	T_f (ideal Transfer Function)	

* $\alpha R_1 \ll kR$ (for maximum ω_p)

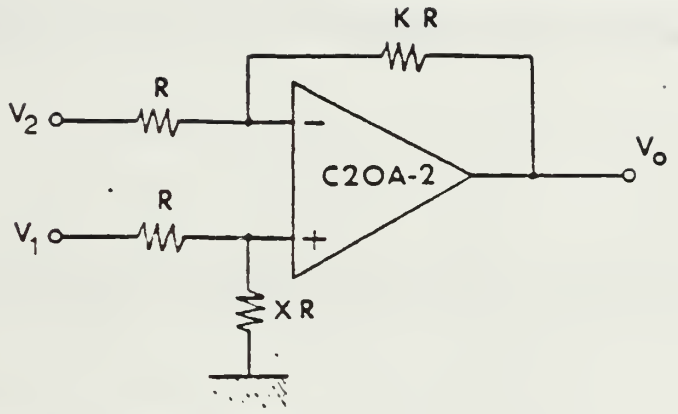

Figure 3.6 Application of the C20A-2 as a Differential Finite Gain Amplifier

where:

$$T_{i1} = X(1 + K)/(1 + X),\ T_{i2} = -K$$

$$w_p = \sqrt{w_1 w_2/(1+K)}\ ,\ Q_p = \sqrt{w_1/w_2(1 + K)}.(1 + \alpha)$$

In the applications given in this section, each of the actual input-output relationships T_a is in the form:

$$T_a = T_i \cdot N/D \qquad (9)$$

where T_i = the transfer function realized assuming ideal OA's

$$N = 1 + as = 1 + s/w_z \text{ (a is zero } (w_z \to \infty) \text{ in some cases)}$$

$$D = 1 + b_1 s + b_2 s^2 = 1 + (s/w_p Q_p) + (s^2/w_p^2)$$

Thus N/d determines the amplitude and phase deviation of T_a from T_i. Also, b_1 and b_2 determine the stability of T_a; a, b_1, and b_2 and consequently w_z, w_p and Q_p, are functions of the circuit parameters which are w_1, w_2 and α. None of the a and b coefficients is realized through differences; this guarantees the low sensitivity of T_a, w_z, w_p and Q_p to the circuit parameters. On the other hand, the b coefficients are always positive (assuming single pole OA model), which guarantees the stability of the transfer

function. From Table 3.1, $\pm$ 5% mismatch in w_1 and w_2 results in a $\pm$ 5% change in w_p and + 2.5% in Q_p. Hence single OA's with mismatched gain bandwidth products within practical ranges can be used without appreciably affecting the stability or the sensitivity of the finite gain realizations.

C. EFFECT OF THE SINGLE OA'S SECOND POLE ON THE STABILITY OF THE C20A'S

In the following, the stability properties of the positive and negative finite gain amplifier realizations using a two pole open loop model of the single OA's is studied. A_1 is assumed equal to A_2. The analysis is simplified without affecting the reliability of the conclusions. This is due to the absence of gain differences in all the gain expressions obtained as seen from equation (3) to equation (6), equation (8) and Table 3.1. Let:

$$A = A_1 = A_2$$

where 1/A is given by:

$$1/A = (1 + s/w_h)(s/A_o w_L + 1/A_o) \qquad (10)$$

$w_h >> w_L$ as shown in Figure 3.7. By applying Routh Hurwitz stability criterion, the necessary and sufficient condition for stability using C20A-1 or C20A-2 is found to be:

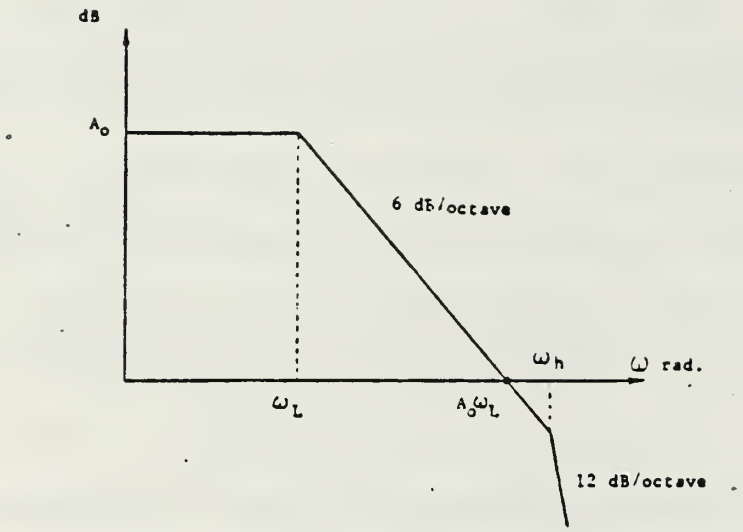

Figure 3.7 Open Loop Frequency Response of a Two-Pole OA

$$(1 + \alpha) < (1 + k)/2 \qquad (11)$$

For C20A-3 the condition is found to be:

$$(1 + \alpha) > \sqrt{(1 + k)} \qquad (12)$$

Also, for C20A-4 the condition is given by:

$$(1 + \alpha) > 4\,(1 + k) \qquad (13)$$

From equation (9), it is desirable to choose α such that Q_p and w_p result in acceptable amplitude and phase deviation in T_a from T_i while satisfying the necessary and sufficient conditions for stability. Table 3.2 gives the values of α required to yield $Q_p = 1/\sqrt{2}$ and $Q_p = 1$ for the realizations in Table 3.1.

The relative useful BW of the different finite gain amplifiers can be obtained by comparing the w_p's in Table 3.2. As w_p increases for a fixed Q_p, both amplitude and phase deviations of T_a from T_i at a given frequency $w(w<w_p)$ decreases. It is clear that C20A-1 and C20A-2 are the two most attractive configurations from the BW and stability considerations.

The BW of a finite gain amplifier realized using a single OA shrinks approximately by a multiplying factor 1/k relative to its unity gain 3 dB BW(w_i). Also the optimum, maximally

TABLE 3.2 VALUES OF α FOR MAXIMALLY FLAT AND FOR $Q_p = 1$, THEIR CORRESPONDING BANDWIDTH AND STABILITY CONDITIONS OF C20A'S IN THE FINITE GAIN APPLICATIONS

$C20A_i$	$1+\alpha$	Q_p	ω_p	Stability Condition for α used
C20A-1	$\sqrt{1+k}$	1	$\frac{\omega_i}{\sqrt{1+k}}$	Satisfied
&				
C20A-2	$\sqrt{\frac{1+k}{2}}$	$\frac{1}{\sqrt{2}}$	(independent of α)	Satisfied
C20A-3	0	$Q_{p_{min}} = \sqrt{1+k}$	$\frac{\omega_i}{\sqrt{1+k}}$	Unsatisfied
C20A-4	$(1+k)$	1	$\frac{\omega_i}{1+k}$	Unsatisfied
	$2(1+k)$	$\frac{1}{\sqrt{2}}$	$\frac{\omega_i}{\sqrt{2}(1+k)}$	Unsatisfied

flat, 3 dB BW using a cascade of two (single OA realization) finite gain amplifiers is obtained when each amplifier has a gain $\sqrt{k}$ to realize an overall gain k. The resulting BW shrinks by $\sqrt{0.44}/\sqrt{k} = 0.66/\sqrt{k}$ relative to w_i. The C20A-1 and C20A-2 circuits BW can be designed to shrink only by a factor of $\simeq 1/\sqrt{k}$ for Q_p=0.707 (maximally flat) and greater than $1/\sqrt{k}$ for Q_p=1 (k>>1). [Ref. 21] In addition, the C20A's require two accurate gain determining components with four in the cascade realization. Figure 3.8 shows the improvement by comparing the BW's obtainable in these different cases.

Comparing the experimental results of negative finite gain amplifier realization [Ref. 20] with those of the single amplifier realizations, illustrates the considerable improvement in the useful BW, without sacrificing any of the single OA attractive features, namely, the low sensitivity to circuit elements and power supply variations, stability and versatility. The sensitivity and stability properties of the differential finite gain amplifier using C20A-2 (Figure 3.6) can be shown to be similar to those derived for C20A-2 in positive and negative finite gain amplification above. To illustrate the usefulness of the derived C20A's a common application is chosen; namely, negative finite gain amplification. The performance of the C20A-1 and C20A-2 in this application is compared with some of the best recently reported negative finite gain realizations.

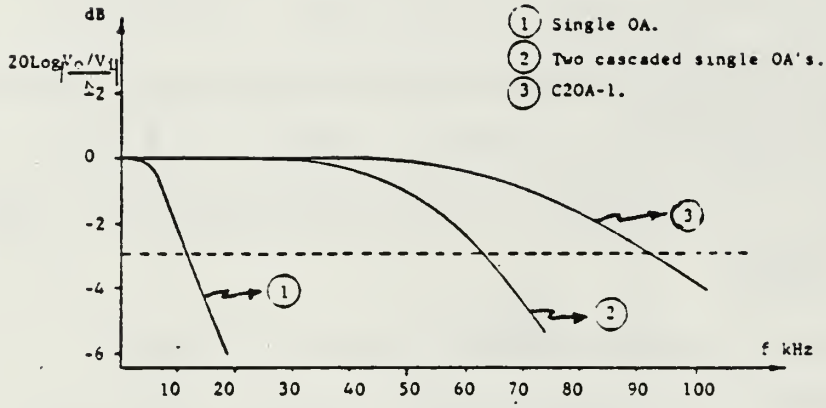

Figure 3.8 Theoretical Frequency Response of Negative Finite Gain Amplifiers Realized Using Single OA, Two Cascaded Single OA's, and C20A-1 for Negative Gain of 100 (assuming OA GBWP = 1 MHz)

[Refs. 22, 23] The results are shown in Figure 3.9 for nominal gains >>1 for practical reasons since as k increases the useful bandwidth shrinks and extending the operating frequencies becomes more important. The results in Figure 3.9 show clearly the excellent gain and phase performance of the proposed realization.

The use of CNOA's is a contribution to the effort to extend the useful operating frequencies of linear active networks. The BW extension is achieved by replacing each of the single OA's in the active realization by a composite OA (CNOA). After this brief introduction to the general technique for the generation of C2OA's (N = 2); examples of C2OA's were discussed concerning their performance characteristics. The C2OA's met stringent performance characteristics for extended BW, stability with one and two pole models, and wide dynamic range, etc. The C2OA's tested in this thesis were C2OA-1, C2OA-2 and C2OA-4. The composite amplifier C2OA-3 was not tested as theory states a value for α can not be found to make C2OA-3 max-flat (avoiding overshoot/undershoot conditions).

Due to the improved active and passive sensitivities of linear networks employing any composite amplifier, an interesting application emerged. The fact that the performances of such networks were found to be less affected by the degradation in active elements parameters, lends itself to radiation hardening applications. In the

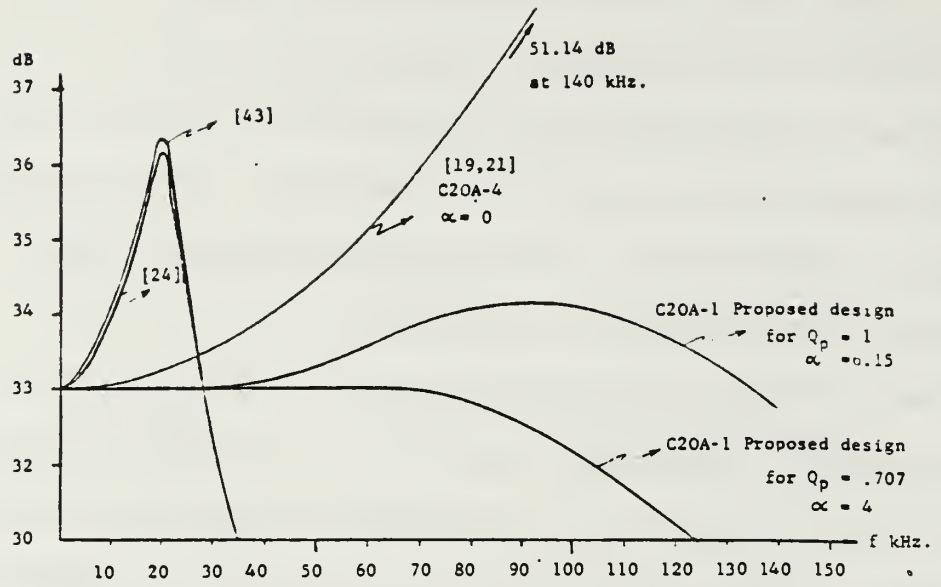

Figure 3.9.a Amplitude Frequency Responses of Negative Finite Gain Amplifiers

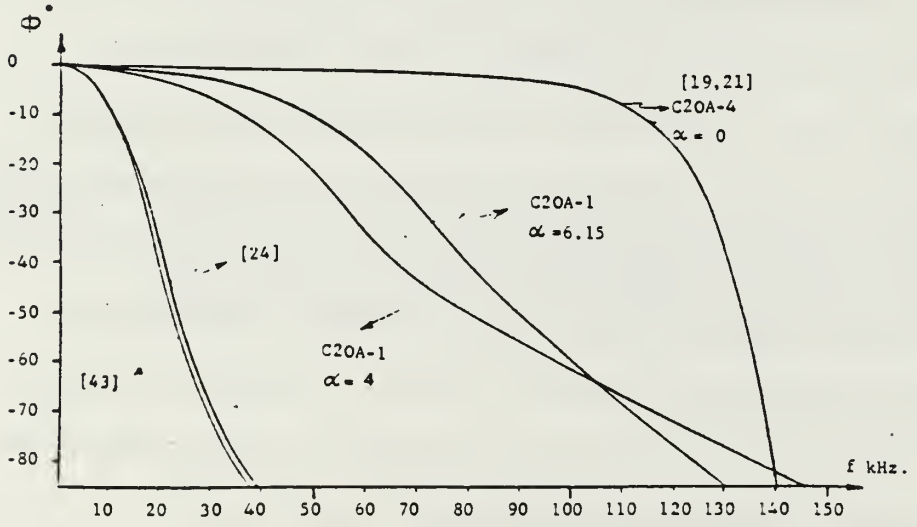

Figure 3.9.b Phase Responses of Negative Finite Gain Amplifiers

Figure 3.9 Comparison of the Negative Finite Gain Amplifiers Using C20A's with the State of the Art Two-OA's Realizations (OA GBWP = 1 MHz)

following chapter, experimental results will demonstrate the improvement of circuit behavior in radiation environments one can gain using composite amplifiers; without the need of hardened devices.

IV. PROCEDURE

A. INTRODUCTION

The purpose of this chapter is to describe the techniques used to gather the results and data which are reported in the following chapter. As the focus of this thesis is on the reaction of operational amplifiers to radiation, the first subject that will be addressed is the sources of that radiation. The primary source was the linear accelerator at the Naval Postgraduate School; the slight modification in calculations to accommodate the situation for the linear accelerator at the Jet Propulsion Laboratory are also addressed. The characteristics of the amplifiers that were measured and the methods of measurement are then introduced to the reader. The effect on bandpass filters incorporating amplifiers were also examined. The procedures used for the room temperature and current annealing experiments were also presented.

B. THE NAVAL POSTGRADUATE SCHOOL LINEAR ACCELERATOR

The linear accelerator (LINAC) at the Naval Postgraduate School was built to emulate those developed at Stanford University in the early 1950's.[Ref. 24] The LINAC is a traveling wave type accelerator; it is a disk loaded circular wave-guide device that has its thirty foot length

separated into three ten foot sections. A series of three klystrons are used to accelerate electrons to relativistic energies of 15MeV to 100MeV (Figure 4.1).

The experiments using the LINAC utilized only 30 MeV electrons, consequently only one Klystron was required. The LINAC pulses sixty times per second with a pulse duration of approximately one microsecond. The target of the electron beam is located inside a vacuum chamber (vacuum held at 1 utorr). The electron beam is focused onto the target by adjusting the magnetic fields of guadrapole magnets. To ensure the beam is of a correct size it is first focused onto a phosphor screen with one-half centimeter reference grid lines. The phosphor screen is attached to an aluminum mounting device (referred to as a ladder) and is aligned above the bakelite board that holds the Bipolar and JFET devices.

A closed circuit television camera displayed a picture of the beam stri-ing the phosphor screen. By using a grease pencil to mark the outline of the beam on the television monitor, a target area was established into which the device to be irradiated was moved by raising the ladder. During these experiments, the beam was shaped to include the entire device package; areas of roughly one-half to three square centimeters. Once the electron beam was properly focused onto the phosphor screen, the

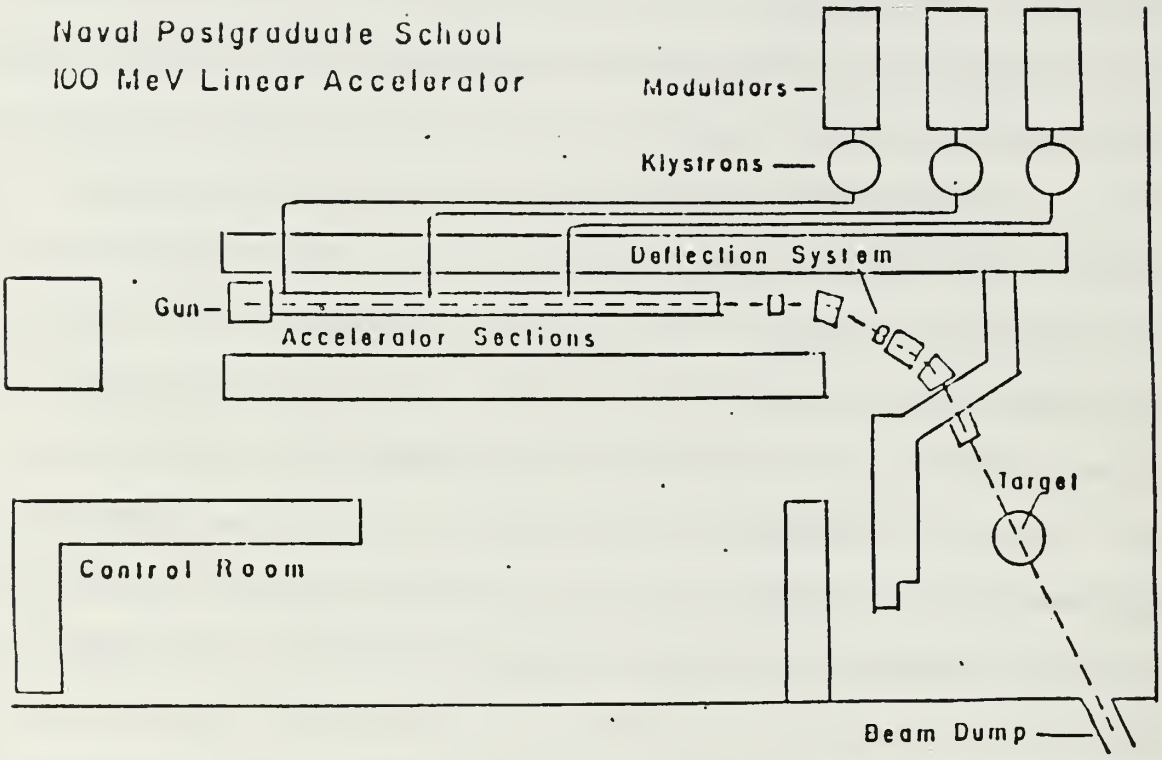

Figure 4.1 LINAC Configuration

beam was turned off and the ladder raised until the device to be irradiated was in the proper position.

For the purposes of this experiment the phosphor screen was considered to be "seasoned", therefore the beam area as shown on the television monitor was considered to be accurate. For a new phosphor screen, the bright spot of the focused electron beam can appear to be 25% larger than the actual beam area.[Ref. 25] For a seasoned beam, the error decreases to zero.

Electron fluence (the number of electrons that pass through a given area) is measured by utilizing a secondary emission monitor (SEM) which is located inside the target chamber. The SEM records the electrons striking it by measuring the voltage developed across a capacitor that is charged by the impacting electrons. The voltage across the capacitor is measured with a voltage integrater circuit. The total number of electrons that have passed through the SEM is determined by:

$$N = Q/q \quad \text{(eqn 1)}$$

N = the total number of electrons

Q = the beam charge

q = the charge per electron

Earlier scattering experiments utilized a Faraday cup to calibrate the large SEM. The large SEM had an electron collection efficiency of 6%,[Ref. 26] The Faraday cup was removed and the large SEM has become the standard for electron beam fluence. The work depicted in this thesis utilized a small SEM. The small SEM was calibrated with the large SEM and determined to be 2.6% efficient at collecting electrons. As the charge relationship for a capacitor is:

$Q = CV$

Q = charge

C = capacitance

V = accumulated voltage on the capacitor

Equation (1) for finding the total number of electrons becomes:

$$N = CV/(0.026q) \quad \text{(eqn 2)}$$

To determine fluence (number of electrons per unit of area), both sides of equation (2) are divided by the beam area (A), and the fluence then becomes:

$$\Phi = N/A = \text{fluence} = CV/(0.026qA) \quad \text{(eqn 3)}$$

Φ = fluence

C = capacitance of capacitor in SEM

A = area of beam

V = voltage on the capacitor

q = charge of an electron

The 30 MeV electron beam energy level was chosen as the LINAC was not as accurate as desired at lower energy levels. Lower energy levels would have been useful for testing of the Bipolar devices. To achieve a proper range of dosage levels for the Bipolar devices, tests were made utilizing the accelerator at the Jet Propulsion Laboratory (JPL) at the California Institute of Technology in Pasadena, California. The JPL accelerator utilized electrons accelerated to a level of 1 MeV. The lower charge of the JPL beam permitted a greater degree of control during testing of the more sensitive Bipolar devices. The 30 MeV energy level was acceptable for the JFET devices and permitted a full range of testing (from no perceptable radiation damage to total destruction).

The dose of radiation energy given to each device was calculated using the following procedures to calculate a value of voltage to be measured on the SEM capacitor for each JFET device. The fluence was established by using equation (3). The fluence was then used in equation (4) to determine the dosage of energy received by the devices expressed in Rads. [Ref. 4]

$R = (1.737 \times 10^{-8})\ ((1/\rho)(dB/dX))$ (eqn 4)

R = Rads for silicon

Φ = fluence

$((1/\rho)(dE/dX))$ = stopping power

The rads (R) reflect the energy deposited in the devices irradiated. One Rad is equal to 100 ergs/gram of energy deposited in the irradiated material. The fluence is calculated with equation (3) based on the voltage measured across the known capacitor in the small SEM and the area of the beam. The stopping power is a function of the material and the energy of the bombarding electrons. The value of the stopping power for silicon and a 30 MeV beam is 1.75 MeV-cm^2/gm. [Ref. 27]

Example calculation:

$\Phi = R/((1.737 \times 10^{-8})((1/\rho)(dE/dX)))$

$R = 1 \times 10^{+4}$ Rads

$C = .05 \times 10^{-6}$ Farads

$q = 1.602 \times 10^{-19}$ Coulombs

V = Volts

A = 1 cm^2

$((1/\rho)(dE/dX)) = 1.75$ MeV-cm^2/gram

$$\phi = \frac{1 \times 10^{+4}}{(1.737 \times 10^{-8})(1.75)} = 3.2897 \times 10^{+11}$$

$$\Phi = \frac{CV}{(0.026qA)}$$

$$V = \frac{\Phi(.026qA)}{C} = \frac{3.2897x10^{+11}(0.026)(1.602x10^{-19})}{(.05x10^{-6})}$$

$$V = 27.37 \text{ m volts}$$

To calculate the fluence for the 1 MeV accelerator at JPL, a stopping power of 1.55 MeV-cm2/gram was used [Ref. 28] in equation (4) with the desired Rad level given. The resulting value for fluence was then used to control the settings on the JPL linear accelerator.

The level of Rads chosen at JPL and NPS was based on indications of previous thesis work and experimental results. At NPS, a Rad level of $1x10^{+5}$ Rads was used as the starting point for the irradiation of the JFET amplifiers. The level of Rads was increased by a factor of 10 until a final level of $1x10^{+8}$ Rads. At $1x10^{+8}$ Rads the JFET amplifiers experienced total destruction by radiation. An interesting result of this process was that the JFETS sustained (with one important exception) only a relatively fixed range of reduced performance as the radiation was increased in the LINAC. The level of damage remained in a general narrow range until the Rad level reaches a limit that causes the final destruction of the device.

An extra test at $3.33x10^{+7}$ Rads was executed to verify that the damage level remained in a fairly stable region until failure occured. The test at $3.33x10^{+7}$ Rads verified that conclusion. On the $3.33x10^{+7}$ Rads test one of the JFET amplifiers was completely destroyed while the other survived to show a lose of performance within the range of loses recorded during pervious experiments. As the primary purpose of this thesis is a comparison of composite amplifier to single amplifier performance; further testing to more precisely define a range of expected damage is left for future researchers. The one test where damage was sustained by a JFET outside the general range of damage developed by these experiments occured at $1x10^{+6}$ Rads. The results from this test were particularly useful for comparing the performance of a damaged single amplifier to that of a damaged composite amplifier and will be elaborated on in that section of this thesis that compares the changes in their 3 dB levels after irradiation.

The Rad levels at JPL were advanced by a factor of 5 vice 10 as the Bipolar devices were expected to be more sensitive to radiation damage. The Bipolar devices also exhibited a tendency to sustain damage within a certain range up to the point where a drastic change occured in the performance of the device (destruction for the JFETS). For the Bipolar devices, the final level of change due to radiation damage was either destruction (as with the JFETS)

or a drastically increased level of performance. The increase in performance consisted of an increase in the 3 dB bandwidth of single amplifiers by up to 7.59:1. The dramatic increase in bandwidth for Bipolar devices due to radiation also presents an interesting subject for further research as a possible means of greatly increasing the performance of electrical components without changing their basic design.

C. HALF POWER POINT

The primary trait that was evaluated/compared for both the single and composite amplifiers was the half power or 3 dB point. The 3 dB point was measured prior to irradiating the devices in the single and composite configurations; after irradiation the 3 dB points were once again measured for both single and composite amplifiers.

The half power (or 3 dB point) occurs when the output power of the amplifier has dropped to one half its original value (hence 3 dB point as 10 log .5 = 3 dB). Power is a function of voltage squared, therefore when the output voltage reaches approximately 5/7 of its original value the power will be half its original value (as (5/7) squared is roughly 1/2).

The process used to measure the 3 dB point was to set the input frequency low enough to ensure that the voltage gain of the amplifier was not affected by the frequency,

and to then adjust the oscilloscope to have the output wave form cover seven verticle voltage gradients (peak to peak voltage of a sine wave). The frequency was then increased until the wave form only covered 5 vertical voltage gradients. At this point, the output voltage is 5/7 of its original value and the power is 5/7 squared or approximately one half the original power. Consequently, our frequency reading at this point is the half-power or 3 dB frequency.

It is the 3 dB point that is being used as the primary measure of performance. The comparison of 3 dB points is made between single and composite amplifiers, both with and without radiation damage.

For the single amplifier, the 3 dB point is an uncomplicated matter of measuring that frequency at which the output voltage has reached 5/7 of its original value. See Figure 4.2 for the diagram of the circuit used to measure the 3 dB point for single as well as composite amplifiers. In both cases three values of finite gain k were used to achieve a high, medium, and low gain measure of performance. The values of k were the same for both single and composite amplifiers to achieve a measure of performance at the same gain levels.

In the case of the composite amplifier configurations, another factor had to be considered in the measuring of the 3 dB point; it was necessary to ensure that the output of the amplifier was in a max-flat configuration. By adjusting

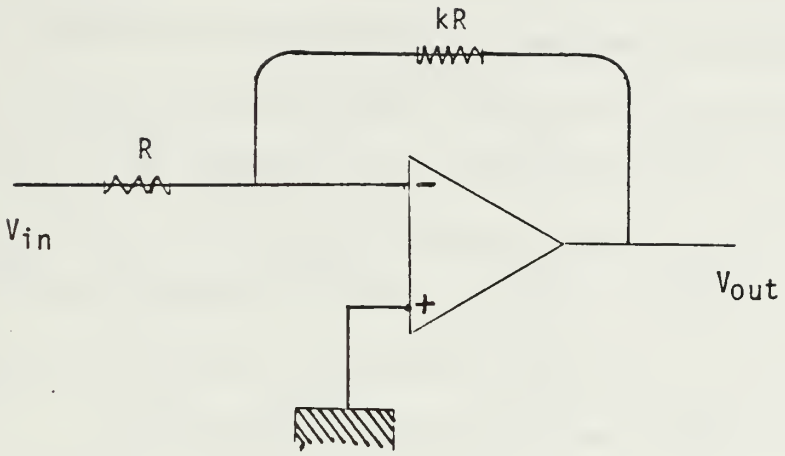

Figure 4.2 Circuit for Measuring 3dB Points

the value of alpha to properly balance each k value, a max-flat configuration is reached when the gain characteristic of the composite amplifier remains at a constant level while the frequency is increased until the 3 dB point. The composite amplifier will then start to lose its gain as the frequency increases until it reaches the 3 dB point. The object is to avoid a sudden increase in gain (overshoot) just prior to the 3 dB point and its associated drop in voltage gain. It is also desired to avoid a too rapid decent in gain prior to the 3 dB point (undershoot).

The method used for each of the three composite amplifiers was to set a desired value of k (which also sets the gain for the composite amplifier) and then adjust alpha through a range of values that permit a steadily decreasing amount of overshoot. When the alpha value is reached where the overshoot has just disappeared prior to the steady reduction in gain due to the 3 dB point; then the alpha value for max-flat operation has been determined. Figures 4.3 and 4.4 give a comparison between calculated and experimentally determined values for alpha that produce a max-flat performance. The calculated values of alpha were the result of operations as shown in Figure 4.5.

While it was not expected to achieve max-flat operations for a gain of 100 (k = 100), max-flat operations were eventually achieved for C20A-4 at k = 100. The actual values for alpha were closer to the calculated values of

gain	k* = 100		k=24		k=15	
	α_1^*	α_2	α_1	α_2	α_1	α_2
C20A-1	6.105	**	2.535	5.535	1.828	3.528
C20A-2	6.105	**	2.535	7.535	1.828	3.828
C20A-4	201	3.4 Meg ohms	49	759	31	631

Alpha 1 = calculated value

Alpha 2 = actual value

* = all values of k and alpha are in kilo-ohms unless indicated otherwise

** = could not achieve max-flat operations at k = 100 as expected [Ref. 29]

Figure 4.3 Alpha Values Calculated vs. Actual (for JFET Devices)

gain	k* = 100		k=24		k=15	
	α_1^*	α_2	α_1	α_2	α_1	α_2
C20A-1	6.105	**	2.535	2.500	1.828	1.600
C20A-2	6.105	**	2.535	2.435	1.828	1.428
C20A-4	201	1.8 Meg ohms	49	1 Meg ohm	31	400

Alpha 1 = calculated value

Alpha 2 = actual value

* = all values of k and alpha are in kilo-ohms unless indicated otherwise

** = could not achieve max-flat operations at k = 100 as expected [Ref. 29]

Figure 4.4 Alpha Values Calculated vs. Actual (for Bipolar Devices)

C20A-1 $Q=\frac{(1+\alpha)}{\sqrt{1+k}}\sqrt{\frac{1}{z}}$ $\alpha=(.707)(\sqrt{1+k})-1$

C20A-2 $Q=\frac{(1+\alpha)}{\sqrt{1+k}}\sqrt{z}$ $\alpha=(.707)(\sqrt{1+k})-1$

C20A-4 $Q=\sqrt{\frac{(1+k)}{(1+\alpha)}z}$ $\alpha=\frac{(1+k)}{.5}-1$

Q = .707 to achieve max-flat operations [Ref. 29]

w1 = bandwidth of amplifier in position A1 for k

w2 = bandwidth of amplifier in position A2 for k

Z = w1/w2, generally w1 and w2 were essentially the same, therefore for these calculations Z = 1

Figure 4.5 Calculations for the Value of Alpha

alpha for the bipolar devices than for the JFET devices; both JFET and bipolar amplifiers generally followed the expected pattern of decreasing value for alpha as indicated by the calculated values of alpha.

D. SLEW RATE

Another area that was evaluated for the affects of radiation was the slew rate. The slew rate is defined as the maximum rate of change of the output voltage, with respect to time, that the amplifier is capable of producing [Ref. 30]. Slew rate is normally measured in volts per microsecond. The method of measuring slew rate utilized in this research was to apply a square wave to the input of the circuit in Figure 4.6. The gain of the circuit is one, the affect of the amplifier on the wave was to alter its shape from a square to a truncated triangular wave form. The slope of the sides of the output wave form gives the slew rate. The slew rate was measured prior to irradiating the devices and after the devices were exposed to radiation. The slew rate was always measured on the trailing edge of the wave form. The composite amplifier follows the single amplifiers that form its components for slew rate, only the slew rate of single amplifiers was measured during this research.

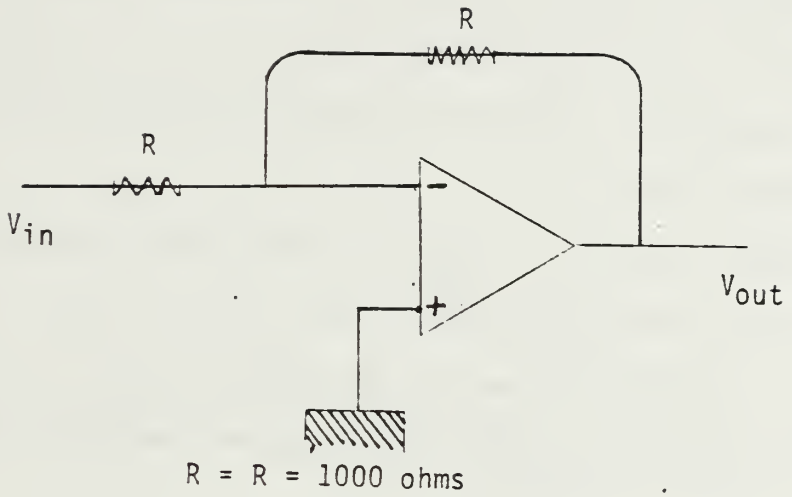

Figure 4.6 Circuit for Measuring Slew Rates

E. BANDPASS FILTER

Another area of research was an inquiry into the affects on the characteristics of bandpass filters (BPF) when they are exposed to radiation. The affects on BPF's were examined for both single and composite amplifiers; see Figure 4.7 for the diagram of the circuit used for the BPF. The composite amplifier used for the BPF was the C20A-4 (Figure 4.8).

The basic characteristics of the single/composite amplifier BPF's were measured prior to and after radiation. The basic characteristics of the BPS measured in this experiment were: central frequency, bandwidth, and "Q" factor.

The central frequency is defined as the frequency at which the filter achieves its highest gain [Ref. 30]. To determine that frequency experimentally, a sine wave was used as the input to the circuit on Figure 4.7. The output of the circuit was then displayed on an oscilloscope. The frequency of the input was adjusted until the output wave form had achieved its highest amplitude; that frequency was then designated as the central frequency.

The bandwidth of the frequency specifies the band of frequencies that the bandpass filter will allow to pass without more than 3 dB of attenuation [Ref. 30]. It is the lower and upper 3 dB points of the BPF output frequency spectrum that determine the size of the bandwidth. The

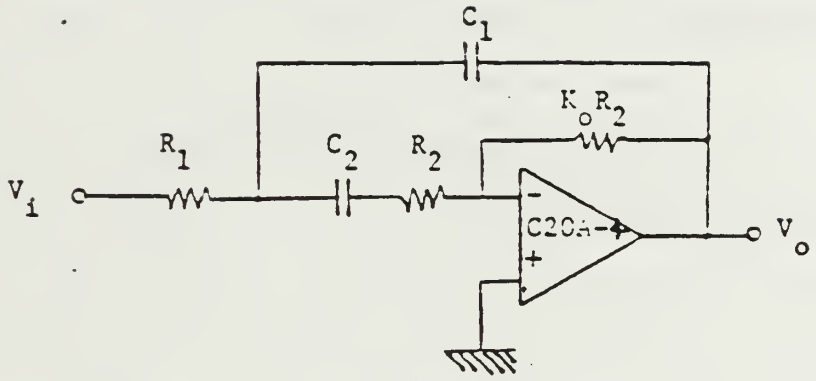

$R_1 = R_2 = 1000$ ohms

$\alpha = 535$ ohms

$C_1 = C_2$

$K_o = 80$

Figure 4.7 Bandpass Filter Using Single QA's or C20A-4

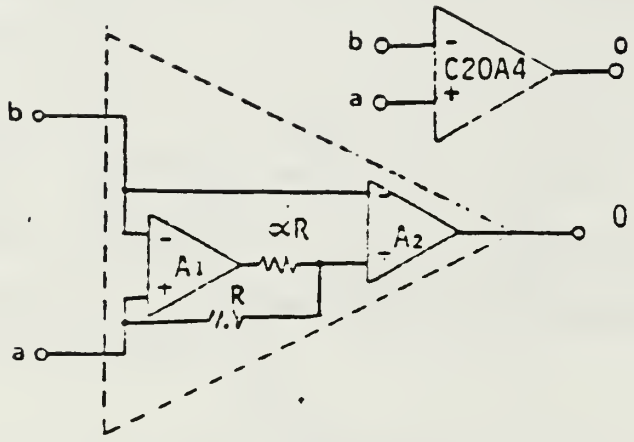

Figure 4.8 C20A-4 Composite Operational Amplifier

procedure used to measure the bandwidth consisted of first locating the central frequency, then finding the upper and lower 3 dB points. Once the central frequency was located, the oscilloscope was adjusted until the wave form of the output covered seven vertical gradients. The frequency of the intput was then adjusted until the output waveform only filled five gradients; indicating the frequency for the 3 dB point had been reached. The difference between the upper and lower frequencies for the 3 dB points determined the bandwidth of the filter.

The final factor is the "Q" factor of the filter. The Q factor is determined by dividing the central frequency by the bandwidth. The Q factor indicates how selective the BPF is; the higher the Q, the smaller the bandwidth and hence the narrower the filter. A high Q value indicates a more selective filter than a low Q value.

Two central frequencies were used to evaluate the effects of radiation on active filters utilizing amplifiers. The two central frequencies permitted evaluation of radiation damage effects at different frequency ranges for the BPF circuits. The theoretical value for the first frequency is:

fo = central frequency

R = resistance = $1 \times 10^{+3}$ ohms

C = capacitance = 300×10^{-12} farads

k = 80

$$fo = 2\pi(1x10^{+3})(300x10^{-12})\sqrt{1+80}$$

$$fo = 58.9x10^{+3} \text{ Hz}$$

The second frequency was achieved by reducing the capacitance to $150x10^{-12}$ farads. Halving the value of the capacitance was achieved by placing two 300 pf capacitors in series to achieve the same results as using a 150pf capacitor. The second frequency was:

$$fo = 117.8x10^{+3} \text{ Hz}$$

The theoretical value for Q is found from:

$$Q = \frac{\sqrt{1+k}}{3} = \frac{\sqrt{1+80}}{3} = 3$$

The radiation damage effects when BPF's are designed with amplifiers was studies for the JFET devices. The JFET devices were used since they were irradiated on the LINAC at NPS and the time was then available to conduct more extensive testing. As the time for testing of the Bipolar devices at JPL was more limited, the BPF filters reactions to radiation was not tested at JPL.

F. ANNEALING

The effects of two types of annealing were examined during the course of the radiation experiments. The first method of annealing was room temperature annealing. The

characteristics of the single and composite amplifiers were measured prior to irradiation and at set intervals up to a week after irradiation of the devices. The object of the measurements was two fold: first to reflect immediate radiation damage and second to record the extent to which the devices continued to deteriorate or recovered with time.

The second method of annealing was an attempt to generate a recovery of the devices capabilities by heating the devices with a constant current (as opposed to an oven). The value of current annealing is that current annealing is a possibility in space; oven annealing would not be very practical (i.e., for an orbiting satellite). For the current annealing experiments two devices were tested. Each device had its output grounded and its input connected to +13 volts causing a constant current to flow through the device. The devices characteristics were measured at different intervals until they finally burned out.

V. RESULTS

A. SLEW RATES

Slew rates were investigated for both JFET and bipolar amplifiers. In general, the slew rates of JFET amplifiers suffered more degradation as the radiation levels were increased during the tests than the bipolar amplifiers. For both types of amplifiers, the slew rates continued to degrade over the period of time that measurements were taken after subjecting the amplifiers to radiation.

The JFET slew rate at the lowest radiation level degraded at the slowest rate and took the longest period of time to reach its lowest value (1 week). The fastest and most complete degradation occurred at the higher radiation levels. In the case of $3.33 \times 10^{+7}$ Rads, one of the JFET devices was completely non-functional when tested immediately after being irradiated.

For the bipolar devices the tests were focused on reaching a point where radiation caused a significant change in the 3 dB frequencies. Consequently, the lower levels of radiation damage were not examined extensively. The bipolar tests were limited by the time available on JPL's linear accelerator. The level of damage to the devices was monitored after each exposure to radiation to find the best level to demonstrate the difference between

single amplifier and composite amplifier performance. When a desired level of radiation damage/change was found (at $5 \times 10^{+6}$ Rads), the amplifiers were tested extensively to determine their operating characteristics over time.

The slew rate experiments for the bipolar devices produced interesting results. It was expected that radiation damage patterns as evidenced by the JFET's would be repeated for the bipolar devices. Instead of a steadily increasing level of degradation of slew rate with increasing radiation; the opposite pattern was noted during the bipolar device experiments.

For the bipolar amplifiers, the slew rate degraded beyond the level of the JFETs for the lower range of $5 \times 10^{+4}$ Rads to $1 \times 10^{+6}$ Rads. The level of degradation was 90%! Once the $5 \times 10^{+6}$ Rads level was reached the level of slew-rate degradation improved greatly to a maximum of only 50%. At $5 \times 10^{+6}$ Rads the bipolar amplifiers also more closely followed the JFET amplifier performances during which the total reduction in slew-rate occurred over a longer period of time (1 week).

The unusual performance described in the above paragraph would be a good point of departure for an evaluation of the physics involved in the irradiation process. The unusual slew-rate degradation would be of particular interest if it could be studied under conditions that approximate space. By using space conditions and energy levels for the

bombarding particles to be expected in space, it should be possible to predict the long term effects on the slew-rate of linear and digital devices in space. The knowledge of spcific data regarding slew-rate changes under radiation could be useful for any digital design that is primarily intended for high radiation areas. Such specific slew-rate investigation is beyond the scope of this thesis.

The evaluation of slew-rate under radiation served two basic purposes for this thesis: one, to verify that radiation induced changes were in fact occurring; and two, to search for an obvious radiation level to slew-rate change relationship.

The first purpose was well served as 3 dB frequencies often did not change dramatically; and it was the definite change in slew-rate that served to verify that radiation damage had in fact occurred.

The secondary purpose of investigating slew-rate changes was that it provided interesting data about the apparently unpatterned changes in slew rate as a result of exposure to radiation. The data provided, while very thought-provoking does not lead to straight-forward conclusions but rather to further, protracted investigation outside the sphere of this thesis.

No effort was made to compare slew-rates for composite and single amplifiers, as composite amplifiers take on the

slew-rate of the component amplifiers. Consequently, composite amplifiers would have the same slew-rate as the component single amplifiers.

B. THE 3 dB FREQUENCY BANDWIDTHS FOR SINGLE AND COMPOSITE AMPLIFIERS

The major focus of this thesis is to compare the operational performance of radiation damaged single amplifiers to radiation damaged composite amplifiers. The primary means of comparison chosen was the 3 dB frequencies for the single and composite amplifiers. It was expected that for both non-radiated and irradiated states the composite amplifiers would have higher 3 dB frequencies. It was also expected that the composite amplifiers would reflect radiation damage in their 3 dB frequencies at a slower rate than single amplifiers; the 3 dB frequency would not decrease as quickly for composite amplifiers as for single amplifiers.

For the JFET amplifiers these expected results were found to be true; the bipolar amplifier experiments, however, had an unusual result. The bipolar amplifiers evidenced a slow decrease in 3 dB frequencies with increasing radiation until the $5 \times 10^{+6}$ Rads level was reached in the experiments. At that point, the 3 dB frequencies for both single and composite amplifiers increased dramatically. For some of the JFET amplifiers there were slight increases in 3 dB frequencies for short periods of time; the increases for the JFETS were

very small and of very short duration when compared to the bipolar devices. However, the general performance relationship of composite and single amplifiers remained as expected (with composite amplifiers out performing single amplifiers).

The comparison of single FJET amplifiers to composite amplifiers followed the general expectations of how the two types of amplifier perform. The single JFET amplifiers showed a steady decrease in 3 dB frequencies (with one exception at $1 \times 10^{+6}$ Rads) as the radiation energy was increased. The damage to the single amplifiers appeared to stay in a definite range until the amplifiers reached a point of total failure (Figure 5.1). The exception to this general trend occurred at $1 \times 10^{+6}$ Rads where one single amplifier (E1) experienced a much larger drop in 3 dB frequency than shown by the other single amplifiers tested at all radiation levels. The amplifiers that were tested at $1 \times 10^{+6}$ Rads will be examined in detail since the large deterioration in performance of E1 permits the clearest comparison of single amplifiers performance to composite amplifiers performance.

The single amplifier (E1) at $1 \times 10^{+6}$ Rads lost 54% of its 3 dB frequency vice the 23% loss that was the maximum loss for all the other single JFET amplifiers (Figure 5.1). The large loss for E1 made the composites formed of E1 and E2 the clearest example of the improved performance of the composite amplifiers. The composite amplifiers not only

	Single			Rads
gain (k)	100	24	15	
Amplifiers				
D	3%	17%	8%	$1x10^5$
E	39%	44%	54%	$1x10^6$
F	11%	23%	10%	$1x10^7$
H	5%	0%	3%	$3.33x10^7$
I	3%	0%	3%	$3.33x10^7$
G	100%	100%	100%	$1x10^8$

Figure 5.1 Maximum Drop in 3 dB Frequencies
JFET

exceeded the single amplifiers in pre-radiation performance, but they also suffered a smaller loss in performance than the component single amplifiers after irradiation.

The composite amplifiers consist of three configurations (Figure 5.2), each configuration will be addressed separately as to its performance in comparison with its component single ampolifiers (E1 and E2).

The first composite amplifier is the C20A-1 composite amplifier (Figure 5.2a). For this composite amplifier; the radiation actually caused the 3 dB frequency to increase from 1% to 14% when E1 was in position A1 of Figure 5.2a. When the more heavily damaged single amplifier E1 was in the A2 position of Figure 5.2a), its influence was more apparent on the composite amplifier and the 3 dB frequencies dropped to 82% of preradiation performance at a gain of 100 and dropped to 69% (worst case) of the composite amplifiers pre-radiation performance at a gain of 15. The drop in performance for the single amplifier E1 was more dramatic; at a gain of 100 it only retained 6% of pre-radiation performance and at a gain of 15 (worst case) it's 3 dB frequency had fallen to only 46% of its pre-radiation performance (Figure 5.3). The effects of radiation on E1 and the subsequent damage to the composite amplifier formed of E1 (E1 in its most influential position A2) and E2 are reported in Figure 5.3. From Figure 5.3 it is clear that the composite amplifier had less degradation in performance

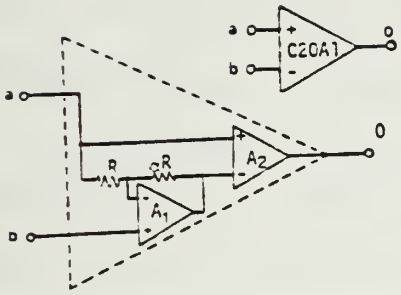

Figure 5.2.a C20A-1

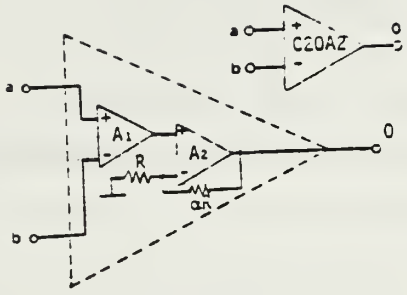

Figure 5.2.b C20A-2

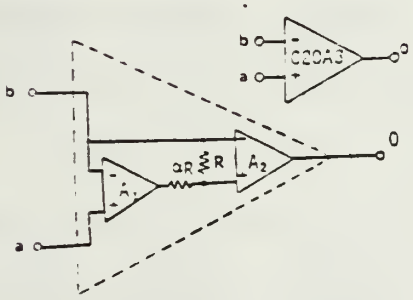

Figure 5.2.c C20A-3

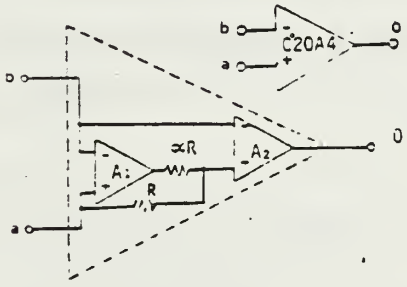

Figure 5.2.d C20A-4

Figure 5.2 The Extended Bandwidth Composite Operational Amplifiers (C20A's)

gain (k)	100	24	15
Single Amplifier (E_1)			
Affect on 3 dB Frequency	-39%	-44%	-54%
Remaining 3 dB Performance	+61%	+56%	+46%
Remaining 3 dB Performance ($\frac{1}{x}$)	1	1	1
	1.64	1.79	2.7
C20A-1 Composite Amplifier (E_1 and E_2)			
Drop In 3 dB Frequency	-18%	-23%	-31%
Remaining 3 dB Performance	+82%	+77%	+69%
Expected 3 dB Performance ($\frac{1}{\sqrt{x}}$)	+78%	+75%	+68%
C20A-2 Composite Amplifier (E_1 and E_2)			
Drop In 3 dB Frequency	-38%	-30%	-37%
Remaining 3 dB Performance	+62%	+70%	+63%
Expected 3 dB Performance ($\frac{1}{\sqrt{x}}$)	+78%	+75%	+68%
C20A-4 Composite Amplifier (E_1 and E_2)			
Drop In 3 dB Performance	-46%	-54%	-55%
Remaining 3 dB Performance	+54%	+46%	+45%
Expected 3 dB Performance ($\frac{1}{\sqrt{x}}$)	+78%	+75%	+68%

Figure 5.3 Radiation Damage Results
Worst Case JFET

than the single amplifier (E1). The composite amplifiers operating at $1/\sqrt{x}$ of its pre-radiation performance; while the single amplifier operated at 1/x of its pre-radiation performance.

Theory indicates that where a single amplifiers' performance is reduced to 1/x of its original performance; the composite amplifier that employs such single amplifier will suffer a performance reduction of $1/\sqrt{x}$ of its original capability. From the results reported in Figure 5.3 (which depicts the worst degradation of performance for both single and composite amplifiers) it is clear that the measured results for the C20A-1 composite amplifier support the basic theory. The reduction in capability of the C20A-1 composite amplifier occurs only when the more heavily damaged single amplifier is in the dominant position A2.

Comparing C20A-1 to its component amplifiers prior to irradiation (Figure 5.4) illustrates the difference in pre-radiation performance very clearly. The composite amplifier has a larger 3 dB frequency than its component amplifiers by a factor of 3.33:1 to 5.32:1. Depending on the gain level chosen, the composite amplifier has a 3 dB frequency that can be more than five times as large as its best component amplifier (Figure 5.4). Consequently, it has more capability to resist radiation damage than its components; and when the composite does lose capability it does so at a slower rate than its components.

gain (k)	100	24	15
Single Amplifier (15)	9.7	41.0	65.0
C20A-1	61.0	170.0	185.0
C20A-1 to 15	6.7:1	4.47:1	3.08:1
C20A-2	84.2	195.0	222.0
C20A-2 to 15	8.68:1	4.76:1	3.42:1
C20A-4	9.62	40.0	64.5
C20A-4 to 15	1.06:1	1.05:1	1.08:1

Figure 5.4 Non Irradiated Performance
Bipolar

The results of evaluating E1 and E2 in the C20A-2 configuration closely follow the evaluation for C20A-1, except that the amplifier in position A1 of Figure 5.2b dominates the composite amplifier. The 3 dB frequency performances for gains of 24 and 15 were within 5% of calculated values. Only the 3 dB frequency for the high gain of 100 had a difference of 16% from the calculated performance, a situation that is off-set by the general performance of C20A-2. While C20A-2 did not follow theory as close as C20A-1, the nonradiation 3 dB frequencies for C20A-2 were as much as 8% higher than the nonradiation values for C20A-1. Additionally, roughly half the post radiation test values for 3 dB frequency were higher for C20A-2 than for C20A-1.

On balance, it would appear, the two composite circuits performed on roughly an equal footing. Further research into the performance of C20A-2 could yield enough performance data to make it possible to design devices that could use its higher 3 dB frequency characteristics to good advantage.

The composite amplifier C20A-4 (Figure 5.2d) is primarily used in filtering applications since it was designed for maximum phase compensation; consequently it is not performing purely as an amplifier, and its performance does not reflect the performances of C20A-1 or C20A-2. The preradiation performance of C20A-4 does reflect an increased 3 dB

frequency by at least 10% and that the amplifier in position A2 of Figure 5.2d dominated the function of the composite amplifier. Once C20A-4 was exposed to radiation its performance was essentially the same as the single amplifier occupying the A2 position of Figure 5.2d.

The pre-radiation performance of the bipolar amplifiers supported the findings for the JFET amplifiers in that the performance of the composite amplifiers greatly exceeded the performance of the single amplifiers.

For the C20A-1 and C20A-2 composite amplifiers, which are designed to primarily function as gain amplifiers, the composite amplifiers out performed the single amplifiers. The two composite amplifiers composed of bipolar transistors exceeded the JFET performance for the higher gain of 100 (Figures 5.3 and 5.4); but were below the JFET performances at gains of 24 and 15. The C20A-4 composite amplifiers performed at roughly the same level for both bipolar and JFET amplifiers. (Figures 5.3 and 5.4)

The 3 dB frequency responses of the irradiated bipolar amplifiers followed an expected slow decline in value until the radiation reached the $5 \times 10^{+6}$ Rads level. At this point, the 3 dB frequency did not decrease but in fact greatly increased over its original value. The increase in 3 dB frequencies was evident in both the single and composite amplifiers (Figures 5.5 and 5.6). While both

gain (k)	100	24	15
Single Amplifier (15)	9.7	41.0	65.0
C20A-1	61.0	170.0	185.0
C20A-1 to 15	6.7:1	4.47:1	3.08:1
C20A-2	84.2	195.0	222.0
C20A-2 to 15	8.68:1	4.76:1	3.42:1
C20A-4	9.62	40.0	64.5
C20A-4 to 15	1.06:1	1.05:1	1.08:1

Figure 5.5 Non Irradiated Performance
Bipolar

gain (k)	100		24		15	
	A	B	A	B	A	B
Test 1	0	295%	0	237%	0	241%
24 Hours	0	553%	0	710%	0	759%
48 Hours	0	509%	317%	636%	315%	667%
1 Week	0	509%	326%	618%	326%	644%

Figure 5.6 Single Bipolar Amplifier Increases of 3 dB Frequency with Radiation (fourteen)

the single and composite amplifiers increased their 3 dB frequencies, the composite amplifiers increased in capability by a higher percentage (Figures 5.5 and 5.6).

The increase in the performance of the bipolar amplifiers was not an expected event. The performance actually increased in two areas: the slew rates had less radiation damage than at lower levels of radiation; the 3 dB frequencies increased over the pre-radiation performance (Figures 5.7 and 5.8). The composite amplifiers generally performed as well or better than the best increase of the component amplifiers. However, the dramatic increase in 3 dB frequencies for the bipolar devices at $5 \times 10^{+6}$ Rads is particularly significant because the stable (one week after test) slew rate performance was as little as 19% lower than the preradiation performance (Figure 5.9). In fact the total performance of the single component amplifiers of composite amplifier 14 at $5 \times 10^{+6}$ Rads had a 3 dB frequency increase as high 6.18:1 at a cost of the slew rate dropping to only 74% of 81% of its preradiation value. It would appear that it should be possible to design circuits that allow for the slower slew rates while utilizing the six fold increase in 3 dB frequencies. Equally interesting was a short improvement in slew rate (5% faster) that occurred at the 48 hour point after the radiation test for composite amplifier 14. The brief improvement in performance at 48 hours, and the obvious differences in final post radiation

BIPOLAR (fourteen)

Best Case

gain (k)	100	24	15
C20A-1	0.0	760.0	780.0
Rad to Non Rad	0.0	608%	578%
C20A-2	0.0	880.0	960
Rad to Non Rad	0.0%	755%	739%
C20A-4	34.0	165	275
Rad to Non Rad	472%	585%	622%

Figure 5.7 Radiation Changes

Device	Rads	Remaining Slew Rate
5A	$5x10^4$	8.7%
5B	$5x10^4$	8.7%
6A	$1x10^5$	9.6%
6B	$1x10^5$	9.7%
8A	$5x10^5$	10.0%
8B	$5x10^5$	9.9%
10A	$1x10^6$	9.0%
10B	$1x10^6$	8.9%

Figure 5.8 Bipolar Slew Rate Performance

Device	14A	14B	15A	15B
Time of test				
Test 1	97.1%	78.6%	54.8%	0.0%
24 hours	0.0%	76.2%	54.8%	0.0%
48 hours	105.0%	76.2%	51.6%	47.5%
1 week	74.0%	81.0%	48.4%	49.2%

Figure 5.9 Bipolar Remaining Slew Rate at $5x10^6$ Rads

slew rates for composite amplifiers 14 (74% to 81%) and 15 (48.4% to 49.2%); indicate that further research at more finely tuned radiation levels is needed, but it may be possible to produce something near to a "super" single amplifier. The irradiated "super" amplifier could retain nearly all of its slew rate, or even improve its slew rate; while it simultaneously increased its 3 dB frequency by 6 fold. The fascinating improvement in performance at the $5 \times 10^{+6}$ Rad level is left to future research in the physics of silicon devices to explain.

C. BANDPASS FILTERS

The JFET amplifiers were used to examine the performance of bandpass filters (BPF) after they had been exposed to radiation. Two different central frequencies were utilized in the BPFs to gain a broader test range of the performance of the BPFs. At each frequency, three basic characteristics were measured before and after radiation. The three basic characteristics were: central frequency (f_o), bandwidth (BW) and Q factor (a measure of the selectiveness of the BPF). Each characteristic changed with radiation to some degree; additionally, there were differences in the performances of the single and composite amplifiers. The differences between the two types of amplifiers were particularly evident at the $1 \times 10^{+6}$ Rads level of radiation; these differences will be elaborated upon as a means of further emphasizing the value of composite amplifiers over single amplifiers.

The central frequency is the mid frequency around which the BPF selects frequencies that it will allow to pass through the filter. It is desired to minimize the deviation of the central frequency with radiation exposure.

The single amplifier central frequency showed a maximum change of 5.5% (Figure 5.10 based on the Appendix) for both central frequencies tested. The change in central frequency due to radiation was thus on a relatively small scale.

For the composite amplifiers, the maximum change in central frequency due to radiation was 5.2% (Figure 5.10). The change in composite amplifiers central frequency was both better and worse than the performance of the single amplifiers; the performance varied with the radiation level. In one regard the composite amplifiers did appear to perform better than the single amplifiers. The composite amplifiers appeared to be more consistent in their percentage of central frequency variance than the single amplifiers (Figure 5.10). The central frequencies of the single amplifiers varied after exposure to radiation over a considerably larger range of values than the composite amplifiers.

The change in central frequencies for the single and composite amplifiers were generally small. The greater consistency in variance of the composite amplifier; however, could be important for predicting performance in specific applications of BPFs.

	$f_{calc} = 59 \times 10^3$ Hz				$f_{calc} = 118 \times 10^3$ Hz			
	f_0	BW	Q	Rads	f_0	BW	Q	Rads
Amplifier								
D_1	-3.5	+10.1	+7.3	1×10^5	same	+3.2	+3.0	1×10^5
D_2	+1.2	+4.5	+5.9	1×10^5	+0.3	+5.6	+6.2	1×10^5
D composite	+4.0	same	+4.0	1×10^5	+0.6	+5.8	+6.8	1×10^5
E_1	-2.4	+8.7	+6.6	1×10^6	-5.5	+10.0	+3.8	1×10^6
E_2	same	+3.1	+2.7	1×10^6	-1.8	+0.4	-1.8	1×10^6
E composite 1	+5.2	+11.3	+18.4	1×10^6	+1.2	+6.2	+7.8	1×10^6
2	+4.8	+14.0	+20.4	1×10^6	+0.2	+9.3	+10.1	1×10^6
F_1	-1.2	+6.2	+5.1	1×10^7	+0.7	+4.9	+4.7	1×10^7
F_2	+1.2	+6.2	+8.0	1×10^7	same	+4.0	+6.0	1×10^7
F composite 1	+0.5	+6.7	+7.4	1×10^7	+0.7	+6.0	+7.1	1×10^7
2	+0.5	+6.7	+7.4	1×10^7	+1.0	+6.0	+7.1	1×10^7

all f_0, BW and Q are in % form
f_0 + = higher
BW + = tighter
Q + = higher
1 = D_1 in positions A1
2 = D_2 in positions A1

Figure 5.10 Band Pass Filter Final Performance Change

The bandwidth of the filter is the range ("band") of useable frequencies that the BPF allows to pass with minimum attenuation. It is desireable to have a stable bandwidth, and (depending on the function chosen) it can be desireable to have a highly selective bandwidth.

The stability of the bandwidths of the single and composite amplifiers was generally good, with the single amplifiers having smaller changes in bandwidth after radiation (Figure 5.10). The changes in bandwidth for both amplifiers that did occur had the effect of tightening the bandwidths (Figure 5.10). In this regard, the composite amplifier had the best performance in that the BW of the composites were narrowed by as much as 14% compared to a maximum tightening of 8.7% for the single amplifiers (Figure 5.10).

An advantage of the composite amplifier is the smaller range of values for the changes in BW the composites experience with radiation. In that regard, it appears that the composites will change their BWs to a more easily predicted range (due to its narrowness) of values than the single amplifiers. The combination of greater predictability and more tightening of BW, appears to indicate that the irradiated composite amplifiers could produce more selective (higher Q) BPFs for some applications than single amplifiers.

The "Q" factor is a result of dividing the central frequency by the bandwidth of the filter. The Q thus

indicates the selectivity of the filter; a higher Q indicates a more selective filter.

The irradiated Q values are primarily a function of BW as the BW experiences larger irradiated changes than does the central frequency. Consequently, the Q values of the composite amplifiers behave as did the BWs and are higher and more stable (smaller range of values) than those for the single amplifiers. The maximum change in Q due to radiation was an increase in selectivity by a factor of 20% at a radiation level of $1 \times 10^{+6}$ Rads. As the Q values are a function of central frequency as well as BW, it is not surprising that the maximum change in Q was different from the change for bandwidth.

The difference in performance between the composite and the single amplifiers is clearest at the $1 \times 10^{+6}$ Rads radiation level. While the central frequency performances are about the same, the BW performances are very different; both factors are neatly reflected in the Q factors of the composite and single amplifiers.

The Q values for the single amplifiers indicate a range of change in selectivity from a slight loss (-1.8%) to a small gain (+6.6%) (Figure 5.10). However, the composite amplifiers have a low increase in selectivity of (+7.8%) to a high increase of 20.4%; a significant improvement over the performance of the single amplifiers. Further, the variation range of irradiated values of the composite amplifiers is

1/2 to 1/3 of that for the single amplifiers. The obvious conclusion is that the irradiated composite amplifier produces a significantly better level of performance in a tighter (therefore easier to predict) range of values than the irradiated single amplifier.

Additional radiation research near $1 \times 10^{+6}$ Rads of radiation could produce more information on the extent to which BPFs can be tightened by exposure to radiation. Given the difference in performance between single and composite amplifiers, it is apparent that the composite amplifiers are the best candidates for this research.

D. CURRENT ANNEALING

The result of the current annealing experiment was that the damaged amplifier did not recover any of its capability and that it "burned-out" after it had been passing its maximum current for eight hours. (Figure 5.11) Further research in this area is recommended.

gain (k)	100	24	15
Non Radiation Performance	33.0	155.0	265.0
Port Radiation Damaged	20.5	88.0	150.0
Time of Annealing			
1 hour	20.2	88.0	150.0
2 hours	20.2	88.0	150.0
4 hours	21.5	87.5	150.0
8 hours	0.0	0.0	0.0

Figure 5.11 Current Annealing Single Amplifier (E1)
3 dB Frequencies (all frequencies $x10^3$ Hz)

VI. CONCLUSIONS AND RECOMMENDATIONS

During the course of this thesis the slew rate proved to be a valuable indicator of the level of radiation damage experienced by the amplifiers; however a pattern of damage due to radiation could not be fully developed. It was the primary goal of this research to demonstrate that composite amplifiers were superior to single amplifiers in a radiation damage environment due to their bandwidth characteristics; a goal that was achieved. Finally, the effects of radiation on bandpass filters that were composed of single and composite amplifiers, were evaluated for radiation induced changes.

Regarding slew rate analysis, the JFET and bipolar amplifiers had radically different responses to radiation. The JFET amplifiers had an expected general pattern of increasing loss of slew rate with increasing radiation until the slew rates were totally lost when the device was destroyed. The bipolar amplifiers had a 90% loss of slew rate until a higher radiation level resulted in a loss as small as 19%. As the two types of amplifiers were tested on two different machines and the machines were each operated at different energy levels, a comparison of amplifier types is difficult. However, it is interesting to note that the pattern of JFET slew rate damage was generally the opposite of the bipolar slew rate damage.

The slew rates did fulfill their most basic function of being an indicator that radiation was affecting the amplifiers. The indication of radiation affecting the amplifiers was important as the 3 dB frequency was not as sensitive to the effects of radiation. Consequently, the presence of slew rate change would indicate the effects of radiation while the 3 dB frequency was still close to its preradiation performance. A general pattern of slew rate change with increasing radiation could not be determined by this research. It is clear, however, that a pattern did exist for each type of amplifier/accelerator; and further research could produce a more concrete relationship between slew rate and radiation levels.

It is recommended that further research be conducted specifically in the area of developing a relationship between slew rates and radiation damage. Establishing a correlation to the type of radiation experienced in space or other high radiation environments would make the experiments more meaningful. With correlation to specific use, the testing for slew rate damage under radiation could then become a valuable tool for high radiation use oriented design of digital devices.

The primary focus of this thesis was on the fact that composite amplifiers have larger 3 dB frequencies than single amplifiers. Additionally, composite amplifiers lose their 3 dB frequency at a slower rate than single amplifiers; this

was another major area of testing in this thesis. Both points were proved valid: the 3 dB frequencies of composite amplifiers were shown to be as high as 6 to 8 times larger than those of single amplifiers; the loss of 3 dB frequencies was at a rate of $1/\sqrt{x}$ for composite amplifiers while single amplifiers lost 3 dB frequency at a faster 1/x rate. Consequently, the basic point that composite amplifiers have higher dB frequency than single amplifiers and that that capability is lost at a slower rate was amply demonstrated by this research. The significantly better performance of composite amplifiers makes them the preferred candidate over single amplifiers for operations in a high radiation environment.

In the course of researching the difference in performance between JFET and bipolar amplifiers an interesting result was observed with the bipolar amplifiers. The single bipolar amplifiers that were exposed to one of the higher levels of radiation ($5 \times 10^{+6}$ Rads) actually increased their 3 dB frequencies by a factor of six. While a significant increase in capability instead of the expected loss was of interest in and of itself; the fact that the slew rate stabilized at up to 81% of its preradiation value made these results considerably more interesting. The slew rates had degraded to only 10% of their preradiation levels prior to the test at $5 \times 10^{+6}$ Rads. Consequently, a nearly total recovery of slew rate and a six fold increase of 3 dB frequency was observed.

It is recommended that further study of bipolar amplifiers at 5 x 10^{+6} Rads be made in an effort to determine how much improvement is posisble in an amplifiers performance after being exposed to radiation. An interesting aspect of this portion of the experiment was that the slew rate actually increased over preradiation levels during its transient response prior to settling down at a less-than-preradiation level. The increase in slew rate, as well as 3 dB frequency, indicates that it might be possible to develop a "super" amplifier.

Bandpass filters using single and composite amplifiers were evaluated for the performance of their three basic characteristics before and after radiation. The three characteristics were central frequency, bandwidth and "Q" factor.

The central frequencies for both single and composite amplifiers performed in essentially the same manner; both had a maximum deviation of about 5% from their preradiation levels. The bandwidths for both types of amplifiers became more selective of the center frequencies (narrower) when exposed to radiation. The composite amplifier filter narrows by a factor of up to 14% while the single amplifier only narrowed its bandwidth by a maximum of 8.7%.

The "Q" factor followed the performance of the bandwidths except that the Q indicated that the filter was more selective by a factor of about 20% at 1 x 10^{+6} Rads.

For all three characteristics, the composite amplifier filter experienced a smaller deviation from the preradiation values than the single amplifier filter. Smaller range of change in characteristics for the composite amplifier filter tends to imply that the composite amplifier filter is more stable and its performance would be easier to predict.

It is recommended that research in filter performance be extended at the $1 \times 10^{+6}$ Rads level. At this level, the composite amplifier filter had an increase in selectivity of frequency by about 20%. More detailed research at the $1 \times 10^{+6}$ Rads level should develop the extent to which filter selectivity can be increased by radiation, as well as models for predicting change in selectivity with changes in radiation.

In summation, it can be said that composite amplifiers out perform single amplifiers in a number of ways. The 3 dB frequencies of composite amplifiers are higher and tend to be decreased due to radiation damage at a slower rate than in single amplifiers. Additionally, radiation can actually improve the frequency selectivity of composite amplifier filters to a significant degree. Based on their general performance in this research, a composite amplifier would be greatly preferred over a single amplifier in a high radiation environment.

APPENDIX
RAW DATA
D BPF $1x10^{+5}$ Rads
Single Amplifier
$fo=59x10^{3}$Hz
calculated

	fo	fL	fH	BW	Q	fo	fL	fH	BW	Q
Non Rad	43.5	33.0	55.8	22.8	1.91	42.0	33.5	56.0	22.5	1.87
Test 1	42.0	32.0	54.8	22.8	1.84	42.0	32.0	55.0	23.0	1.83
1 hour	41.0	32.0	55.0	23.0	1.78	41.0	32.0	55.5	23.5	1.75
10 hours	40.0	32.0	55.0	23.0	1.74	40.0	32.0	56.0	24.0	1.67
2 days	42.0	32.5	55.0	22.5	1.87	42.0	32.5	56.0	23.5	1.79
1 week	42.0	34.0	54.5	20.5	2.05	42.5	33.5	55.0	21.5	1.98

Composite Amplifier
$fo=59x10^{3}$Hz
calculated

1

	fo	fL	fH	BW	Q
Non Rad	42.5	34.5	58.5	24.0	1.77
Test 1	42.5	32.0	58.5	26.5	1.60
1 hour	42.5	33.5	58.5	25.0	1.70
10 hours	40.0	33.5	58.5	25.0	1.60
2 days	44.5	34.0	58.2	24.2	1.84
1 week	44.2	34.2	58.2	24.0	1.84

2

Non Rad

Test 1

1 hour

10 hours

2 days

1 week

-All frequencies $x10^{3}$
-For composite 1 and 2 indicate chip in A+ positions of Figure

D BPF x10^{+5} Rads
Single Amplifier
fo= 118x10^{3}Hz
calculated

	fo	fL	fH	BW	Q	fo	fL	fH	BW	Q
Non Rad	77.0	57.0	104.4	47.0	1.64	78.0	57.0	105.5	48.5	1.61
Test 1	76.5	55.5	104.5	49.0	1.56	76.0	55.0	106.5	51.5	1.48
1 hour	77.0	56.5	105.0	48.5	1.59	77.5	56.5	106.5	50.0	1.55
10 hours	76.5	55.0	106.0	51.0	1.50	78.5	57.0	106.5	49.5	1.59
2 days	78.0	58.0	103.5	45.5	1.71	78.5	58.0	105.0	47.0	1.67
1 week	77.0	58.0	103.5	45.5	1.69	78.5	58.2	104.0	45.8	1.71

Composite Amplifier
fo= 118x10^{3}Hz
calculated

1

	fo	fL	fH	BW	Q
Non Rad	84.5	60.5	118.0	57.5	1.47
Test 1	83.0	60.0	116.2	56.2	1.48
1 hour	84.0	60.0	116.5	56.5	1.49
10 hours	84.5	60.0	118.0	58.0	1.46
2 days	84.2	62.0	116.2	54.2	1.55
1 week	85.0	62.0	116.2	54.2	1.57

2

Non Rad

Test 1

1 hour

10 hours

2 days

1 week

-All frequencies x10^{3}
-For composite 1 and 2 indicate chip in A+ positions of Figure

E BPF $x10^{+6}$ Rads
Single Amplifier
$fo=59x10^{3}$Hz
calculated

	fo	fL	fH	BW	Q	fo	fL	fH	BW	Q
Non Rad	42.0	32.5	55.5	23.0	1.83	42.0	32.0	55.0	23	1.83
Test 1	38.5	31.8	52.2	20.4	1.89	39.5	32.1	55.0	22.0	1.72
1 hour	39.5	31.0	53.8	22.8	1.73	39.5	31.5	55.0	23.5	1.68
10 hours	39.0	31.0	53.0	22.0	1.77	39.0	31.0	55.0	24.0	1.63
2 days	40.0	31.0	53.0	22.0	1.82	42.0	32.0	54.5	22.5	1.87
1 week	41.0	32.0	53.0	21.0	1.95	42.0	32.2	54.5	22.3	1.88

Composite Amplifier

fo=59 kHz
calculated

E 1

	fo	fL	fH	BW	Q
Non Rad	42.0	32.2	59.8	27.6	1.52
Test 1	43.2	34.0	58.2	24.2	1.79
1 hour	40.0	32.0	59.0	27.0	1.48
10 hours	39.5	32.2	59.0	26.8	1.47
2 days	44.0	33.5	58.0	24.5	1.80
1 week	44.2	34.0	58.5	24.5	1.80

E 2

Non Rad	42.0	32.2	59.8	27.6	1.52
Test 1	41.5	33.8	58.0	24.2	1.72
1 hour	39.5	32.0	60.3	28.3	1.40
10 hours	39.5	32.0	59.0	27.0	1.46
2 days	43.5	32.0	58.5	26.5	1.64
1 week	44.0	34.2	58.2	24.0	1.83

-All frequencies and bandwidths in kilo hertz.
-For composite 1 and 2 indicate amplifier in A+ position of Figure

E BPF $x10^{+6}$ Rads
Single Amplifier
$fo = 118x10^{3}$Hz
calculated

	fo	fL	fH	BW	Q	fo	fL	fH	BW	Q
Non Rad	78.5	56.2	106.0	49.8	1.58	77.5	56.5	104.5	48.0	1.62
Test 1	75.0	54.5	101.0	46.5	1.61	76.5	56.2	103.5	47.3	1.62
1 hour	75.0	55.0	100.0	45.0	1.67	76.5	57.0	104.0	47.0	1.63
10 hours	74.5	54.2	100.0	45.8	1.63	76.0	56.2	103.5	47.3	1.61
2 days	74.0	54.2	100.0	45.8	1.62	76.0	56.5	102.0	45.5	1.67
1 week	74.2	54.2	99.5	45.3	1.64	76.0	56.0	103.8	47.8	1.59

Composite Amplifier
$fo = 118x10^{3}$Hz
calculated

1

	fo	fL	fH	BW	Q
Non Rad	84.0	59.8	119.0	59.2	1.42
Test 1	84.2	62.2	115.5	53.3	1.58
1 hour	84.0	58.0	123.0	65.0	1.29
10 hours	85.0	60.5	118.2	57.7	1.47
2 days	85.0	62.0	115.0	53.0	1.60
1 week	85.0	61.5	117.0	55.5	1.53

2

Non Rad	84.0	59.8	119.0	59.2	1.42
Test 1	82.5	61.0	115.5	54.5	1.51
1 hour	82.5	57.5	121.0	63.5	1.30
10 hours	84.2	60.2	117.0	56.8	1.48
2 days	84.2	61.5	114.5	53.0	1.59
1 week	84.2	61.8	115.5	53.7	1.57

-All frequencies $x10^{3}$
-For composite 1 and 2 indicate chip in A+ positions of Figure

F BPF $x10^{+7}$ Rads
Single Amplifier
$fo= 59x10^{3}$Hz
calculated

	fo	fL	fH	BW	Q	fo	fL	fH	BW	Q
Non Rad	42.0	32.0	56.0	24.0	1.75	42.0	32.0	56.0	24.0	1.75
Test 1	39.0	31.0	55.0	24.0	1.63	39.0	31.0	55.0	24.0	1.63
1 hour	42.0	33.0	54.5	21.5	1.95	41.8	32.0	55.0	23.0	1.82
10 hours	42.0	32.0	54.5	22.5	1.87	41.5	32.0	55.0	23.0	1.80
2 days	41.0	32.0	54.5	22.5	1.82	41.0	32.0	54.5	22.5	1.82
1 week	41.5	33.0	55.5	22.5	1.84	42.5	33.0	55.5	22.5	1.89

Composite Amplifier
$fo=59x10^{3}$Hz
calculated

1

	fo	fL	fH	BW	Q
Non Rad	44.0	32.0	59.0	27.0	1.63
Test 1	40.0	32.0	59.0	27.0	1.48
1 hour	44.0	33.5	58.2	24.7	1.78
10 hours	44.0	32.0	58.2	26.2	1.70
2 days	43.5	32.5	58.2	25.7	1.69
1 week	44.2	33.0	58.2	25.2	1.75

2

Non Rad	44.0	32.0	59.0	27.0	1.63
Test 1	39.5	31.5	59.0	27.5	1.44
1 hour	44.0	34.0	58.0	24.0	1.83
10 hours	44.0	32.2	58.2	26.0	1.69
2 days	44.0	33.0	58.2	25.2	1.75
1 week	44.2	33.0	58.2	25.2	1.75

-All frequencies $x10^{3}$
-For composite 1 and 2 indicate chip in A+ positions of Figure

F BPF $x10^{+7}$ Rads
Single Amplifier
$fo=118x10^{3}$Hz
calculated

	fo	fL	fH	BW	Q	fo	fL	fH	BW	Q
Non Rad	76.5	55.5	106.0	50.5	1.52	76.5	55.5	106.0	50.5	1.52
Test 1	76.0	55.0	105.5	50.5	1.51	77.0	59.5	100.0	40.5	1.90
1 hour	76.0	56.5	104.5	48.0	1.58	76.5	57.5	103.5	46.0	1.66
10 hours	77.0	56.0	105.8	49.8	1.55	78.0	56.0	106.0	50.0	1.56
2 days	76.5	56.0	104.2	48.2	1.59	77.5	56.0	104.0	48.0	1.62
1 week	77.0	56.5	104.5	48.0	1.60	76.5	56.5	105.0	48.5	1.58

Composite Amplifier
$fo=118x10^{3}$Hz
calculated

1

	fo	fL	fH	BW	Q
Non Rad	84.2	59.9	120.0	60.1	1.40
Test 1	84.0	61.0	117.8	56.8	1.40
1 hour	83.5	61.0	116.5	55.5	1.51
10 hours	84.2	61.0	118.0	57.0	1.48
2 days	84.0	61.0	116.0	55.0	1.53
1 week	84.8	61.0	117.5	56.5	1.50

2

Non Rad	84.2	59.9	120.0	60.1	1.40
Test 1	84.0	61.0	117.5	56.5	1.49
1 hour	84.2	62.0	115.5	53.5	1.57
10 hours	84.2	61.0	117.5	56.5	1.49
2 days	84.0	61.0	116.0	55.0	1.53
1 week	85.0	61.0	117.5	56.5	1.50

-All frequencies $x10^{3}$
-For composite 1 and 2 indicate chip in A+ positions of Figure

H BPF $3.33 \times 10^{+7}$ Rads
Single Amplifier
$fo = 59 \times 10^{3}$ Hz
calculated

	fo	fL	fH	BW	Q	fo	fL	fH	BW	Q
Non Rad	42.2	33.0	55.5	22.5	1.88	42.0	32.5	56.0	23.5	1.79
Test 1	0.0	0.0	0.0	0.0	0.0	41.0	33.0	56.0	23.0	1.78
1 hour										
10 hours										
2 days										
1 week										

Composite Amplifier
$fo = 59.0 \times 10^{3}$ Hz
calculated

1

	fo	fL	fH	BW	Q
Non Rad	44.2	34.0	59.0	25.0	1.76
Test 1					
1 hour					
10 hours					
2 days					
1 week					

2

Non Rad	
Test 1	
1 hour	
10 hours	
2 days	
1 week	

-All frequencies $\times 10^{3}$
-For composite 1 and 2 indicate chip in A+ positions of Figure

H BPF $3.33 \times 10^{+7}$ Rads
Single Amplifier

$f_o = 118 \times 10^{3}$ Hz
calculated

	fo	fL	fH	BW	Q	fo	fL	fH	BW	Q
Non Rad	78.0	57.0	104.5	47.5	1.64	78.0	57.5	105.0	47.5	1.64
Test 1	0.0	0.0	0.0	0.0	0.0	78.0	57.5	106.5	49.0	1.59
1 hour										
10 hours										
2 days										
1 week										

Composite Amplifier

$f_o = 118 \times 10^{3}$ Hz
calculated

1

	fo	fL	fH	BW	Q
Non Rad	84.0	61.0	115.8	54.8	1.53
Test 1					
1 hour					
10 hours					
2 days					
1 week					

2

Non Rad	
Test 1	
1 hour	
10 hours	
2 days	
1 week	

-All frequencies $\times 10^{3}$
-For composite 1 and 2 indicate chip in A+ positions of Figure

I BPF $3.33 \times 10^{+7}$ Rads
Single Amplifier
$fo = 59 \times 10^{3}$ Hz
calculated

	fo	fL	fH	BW	Q	fo	fL	fH	BW	Q
Non Rad	42.0	32.5	56.0	23.5	1.79	41.5	33.0	55.0	22.0	1.89
Test 1	0.0	0.0	0.0	0.0	0.0	41.5	33.5	55.5	22.0	1.89
1 hour										
10 hours										
2 days										
1 week										

Composite Amplifier
$fo = 59 \times 10^{3}$ Hz
calculated

1

	fo	fL	fH	BW	Q
Non Rad	44.2	34.2	58.5	24.3	1.82
Test 1					
1 hour					
10 hours					
2 days					
1 week					

2

Non Rad
Test 1
1 hour
10 hours
2 days
1 week

-All frequencies $\times 10^{3}$
-For composite 1 and 2 indicate chip in A+ positions of Figure

I BPF $3.33 \times 10^{+7}$ Rads
Single Amplifier
$fo = 118 \times 10^{3}$ Hz
calculated

	fo	fL	fH	BW	Q	fo	fL	fH	BW	Q
Non Rad	79.0	57.8	105.5	47.7	1.66	78.0	57.8	106.0	48.2	1.62
Test 1	0.0	0.0	0.0	0.0	0.0	78.0	56.0	106.5	50.5	1.55
1 hour										
10 hours										
2 days										
1 week										

Composite Amplifier
$fo = 118 \times 10^{3}$ Hz
calculated

1

	fo	fL	fH	BW	Q
Non Rad	84.0	61.0	116.0	55.0	1.53
Test 1					
1 hour					
10 hours					
2 days					
1 week					

2

Non Rad	
Test 1	
1 hour	
10 hours	
2 days	
1 week	

-All frequencies $\times 10^{3}$
-For composite 1 and 2 indicate chip in A+ positions of Figure

G BPF x10^{+8} Rads
Single Amplifier
fo=59×10^{3}Hz
calculated

	fo	fL	fH	BW	Q	fo	fL	fH	BW	Q
Non Rad	42.5	32.5	55.5	23.0	1.85	42.2	32.2	54.9	22.7	1.86
Test 1										
1 hour										
10 hours										
2 days										
1 week										

Composite Amplifier
fo=59×10^{3}Hz
calculated

1

	fo	fL	fH	BW	Q
Non Rad	44.0	32.5	58.0	25.5	1.73
Test 1					
1 hour					
10 hours					
2 days					
1 week					

2

Non Rad	44.0	32.5	58.0	25.5	1.73
Test 1					
1 hour					
10 hours					
2 days					
1 week					

-All frequencies x10^{3}
-For composite 1 and 2 indicate chip in A+ positions of Figure

G BPF $x10^{+8}$ Rads
Single Amplifier
$fo=118x10^{3}$Hz
calculated

	fo	fL	fH	BW	Q	fo	fL	fH	BW	Q
Non Rad	78.0	58.2	105.0	46.8	1.67	78.5	58.0	104.0	46.0	1.71
Test 1										
1 hour										
10 hours										
2 days										
1 week										

Composite Amplifier
$fo=118x10^{3}$Hz
calculated

1

	fo	fL	fH	BW	Q
Non Rad	83.0	62.0	115.0	53.0	1.57
Test 1					
1 hour					
10 hours					
2 days					
1 week					

2

Non Rad	84.5	61.8	115.8	54.0	1.57
Test 1					
1 hour					
10 hours					
2 days					
1 week					

-All frequencies $x10^{3}$
-For composite 1 and 2 indicate chip in A+ positions of Figure

D 1 x10^{+5} Rads

Slew Rates volts/microseconds

	D_1	D_2
Non Radiation	19.2	26.25
Test 1	19.5	25.7
1 hour	19.5	23.8
10 hours	19.5	23.8
2 days	17.2	17.9
1 week	15.2	20.0

Single Amplifier 3dB Frequencies
all frequencies x10^{+3} Hz

	D_1			D_2		
Gain (k)	100	24	15	100	24	15
Non Radiation	35.0	168.0	265.0	38.0	185.0	295.0
Test 1	34.5	150.0	260.0	39.0	175.0	290.0
1 hour	36.0	150.0	260.0	40.2	180.0	300.0
10 hours	36.0	150.0	255.0	40.2	190.0	290.0
2 days	34.5	140.0	245.0	38.0	165.0	270.0
1 week	34.2	160.0	245.0	37.0	175.0	280.0

$E \times 10^{+6}$ Rads

Slew Rates volts/microseconds

	E_1	E_2
Non Radiation	25.6	25.0
Test 1	13.5	13.2
1 hour	11.4	11.6
10 hours	10.6	10.6
2 days	10.0	10.0
1 week	10.0	10.0

Single Amplifier 3dB Frequencies

all frequencies $\times 10^{+3}$ Hz

	E_1			E_2		
Gain (k)	100	24	15	100	24	15
Non Radiation	33.0	155.0	265.0	33.0	150.0	242.0
Test 1	36.0	180.0	285.0	34.2	150.0	245.0
1 hour	20.0	90.5	142.0	32.0	142.0	242.0
10 hours	20.0	99.9	150.0	34.0	142.0	242.0
2 days	20.5	86.5	122.0	32.0	125.0	235.0
1 week	20.5	86.5	150.0	33.0	150.0	240.0

$Fx10^{+7}$ Rads

Slew Rates volts/microseconds

	F_1	F_2
Non Radiation	20.8	25.6
Test 1	12.5	17.9
1 hour	13.2	17.9
10 hours	11.4	16.7
2 days	11.4	16.1
1 week	11.4	16.1

Single Amplifier 3dB Frequencies
all frequencies $x10^{+3}$ Hz

	F_1			F_2		
Gain (k)	100	24	15	100	24	15
Non Radiation	35.0	155.0	260.0	35.0	155.0	260.0
Test 1	34.0	140.0	235.0	31.5	142.0	235.0
1 hour	34.0	140.0	240.0	31.5	142.0	235.0
10 hours	34.2	140.0	250.0	33.0	135.0	245.0
2 days	34.2	122.0	240.0	33.0	120.0	245.0
1 week	33.0	142.0	240.0	33.5	145.0	245.0

$G \times 10^{+8}$ Rads

Slew Rates volts/microseconds

	G_1	G_2
Non Radiation	27.8	17.9
Test 1	0.76	7.81
1 hour		
10 hours		
2 days		
1 week		

Single Amplifier 3dB Frequencies

all frequencies $\times 10^{+3}$ Hz

	G_1			G_2		
Gain (k)	100	24	15	100	24	15
Non Radiation	37.0	155.0	275.0	35.8	150.0	270.0
Test 1	35.0	79.5	109.0			
1 hour						
10 hours						
2 days						
1 week						

H $3.33 \times 10^{+7}$ Rads

Slew Rates volts/microseconds

	H_1	H_2
Non Radiation	25.0	23.8
Test 1	5.0	13.9
1 hour		
10 hours		
2 days		
1 week		

Single Amplifier 3dB Frequencies
all frequencies $\times 10^{+3}$ Hz

	1			2		
Gain (k)	100	24	15	100	24	15
Non Radiation	37.0	155.0	270.0	39.0	155.0	290.0
Test 1	0.0	0.0	0.0	37.0	175.0	280.0
1 hour						
10 hours						
2 days						
1 week						

I $3.33 \times 10^{+7}$ Rads

Slew Rates volts/microseconds

	I_1	I_2
Non Radiation	20	21.7
Test 1	0	14.7
1 hour		
10 hours		
2 days		
1 week		

Single Amplifier 3dB Frequencies
all frequencies $\times 10^{+3.}$ Hz

	I_1			I_2		
Gain (k)	100	24	15	100	24	15
Non Radiation	37.5	155.0	280.0	38.2	155.0	290.0
Test 1	0.0	0.0	0.0	37.0	170.0	280.0
1 hour						
10 hours						
2 days						
1 week						

Composite Amplifier 3dB Max Flat Frequencies $1x10^{+5}$ Rads

C20A-1 D

gain (k)	100		24		15	
α	6.105		5.535		3.528	
	1	2	1	2	1	2
Non Radiation	124.0		995.0		1.45M	
1st test	115.0		935.0		1.4M	
1 hour	126.0		1.0M		1.4M	
10 hours	132.0		1.042M		1.42M	
2 days	106.5		1.01M		1.35M	
1 week	116.5		1.01M		1.42M	

C20A-2

gain (k)	100		24		15	
α	6.105		7.535		3.828	
	1	2	1	2	1	2
Non Radiation	103.5		950.0		1.24M	
1st test	110.0		940.0		1.165M	
1 hour	108.5		920.0		1.225M	
10 hours	135.0		1.025M		1.335M	
2 days	130.0		900.0		1.14M	
1 week	108.5		955.0		1.235M	

C20A-4

gain (k)	100		24		15	
α	3.4 $x10^{+6}$ ohms		759		631	
	1	2	1	2	1	2
Non Radiation	41.5		205.0		342.0	
1st test	42.5		205.0		330.0	
1 hour	42.0		205.0		325.0	
10 hours	45.0		205.0		350.0	
2 days	42.5		205.0		330.0	
1 week	40.0		200.0		330.0	

-Unless indicated otherwise k and are K ohms ($x10^{+3}$ ohms)
-1 or 2 indicates amplifier in A1 position on Figures
-All freqs $x10^{3}$ Hz unless followed by M, M=$1x10^{+6}$ Hz

Composite Amplifier 3dB Max Flat Frequencies E x10^{+6} Rads

C20A-1 E

gain (k)	100		24		15	
α	6.105		5.535		3.528	
	1	2	1	2	1	2
Non Radiation	110.0	110.0	825.0	825.0	1.18M	1.18M
1st test	110.0	99.5	942.0	800.0	1.19M	1.035M
1 hour	116.0	90.0	875.0	655.0	1.16M	855.0
10 hours	121.0	92.2	880.0	665.0	1.115M	860.0
2 days	121.0	92.0	895.0	645.0	1.162M	835.0
1 week	118.0	92.0	870.0	635.0	1.165M	820.0

C20A-2

gain (k)	100		24		15	
α	6.105		7.535		3.828	
	1	2	1	2	1	2
Non Radiation	117.0	117.0	985.0	985.0	1.275M	1.275M
1st test	96.0	122.0	740.0	920.0	890.0	1.22M
1 hour	93.5	115.5	720.0	870.0	865.0	1.135M
10 hours	90.0	106.5	720.0	842.0	840.0	1.11M
2 days	84.5	103.0	685.0	830.0	800.0	1.1M
1 week	90.0	110.0	705.0	850.0	830.0	1.12M

C20A-4

gain (k)	100 x10^{+6}		24		15	
α	3.4 ohms		759		631	
	1	2	1	2	1	2
Non Radiation	37.0	37.0	180.0	180.0	302.0	302.0
1st test	35.8	22.0	150.0	110.0	245.0	180.0
1 hour	32.5	19.9	150.0	94.0	245.0	170.0
10 hours	31.5	20.0	141.0	90.0	235.0	155.0
2 days	32.0	20.0	130.0	83.5	235.0	135.0
1 week	32.0	20.0	150.0	86.5	235.0	150.0

-Unless indicated otherwise k and are K ohms (x10^{+3} ohms)
-1 or 2 indicates amplifier in A1 position on Figures
-All freqs x10^{3} Hz unless followed by M, M=1x10^{+6} Hz

Composite Amplifier 3dB Max Flat Frequencies Fx10^{+7} Rads

C20A-1

gain (k)	100		24		15	
α	6.105		5.535		3.528	
	1	2	1	2	1	2
Non Radiation	111.0	111.0	845.0	845.0	1.205M	1.205M
1st test	104.0	104.0	800.0	815.0	1.155M	1.200M
1 hour	104.0	107.0	790.0	795.0	1.155M	1.242M
10 hours	114.0	104.2	880.0	920.0	1.255M	1.300M
2 days	109.5	111.5	800.0	855.0	1.155M	1.290M
1 week	108.5	102.5	830.0	785.0	1.265M	1.290M

C20A-2

gain (k)	100		24		15	
α	6.105		7.535		3.828	
	1	2	1	2	1	2
Non Radiation	111.0	111.0	922.0	922.0	1.165M	1.165M
1st test	98.0	97.0	820.0	800.0	1.070M	1.050M
1 hour	111.5	103.5	875.0	860.0	1.142M	1.100M
10 hours	104.0	100.0	895.0	870.0	1.171M	1.095M
2 days	106.5	103.5	865.0	870.0	1.160M	1.150M
1 week	101.0	102.0	865.0	830.0	1.180M	1.110M

C20A-4

gain (k)	100 x10^{+6}		24		15	
α	3.4 ohms		759		631	
	1	2	1	2	1	2
Non Radiation	38.0	38.0	150.0	150.0	282.0	282.0
1st test	36.5	36.5	162.0	162.0	275.0	275.0
1 hour	34.2	37.0	142.0	165.0	255.0	275.0
10 hours	33.0	37.0	130.0	133.0	255.0	290.0
2 days	37.5	37.0	130.0	130.0	285.0	290.0
1 week	35.0	37.5	150.0	180.0	260.0	285.0

-Unless indicated otherwise k and are K ohms (x10^{+3} ohms)
-1 or 2 indicates amplifier in A1 position on Figures
-All freqs x10^{3} Hz unless followed by M, M=1x10^{+6} Hz

Composite Amplifier 3dB Max Flat Frequencies Gx10^{+8} Rads

C20A-1

gain (k)	100		24		15	
α	6.105		5.535		3.528	
	1	2	1	2	1	2
Non Radiation	115.0	116.5	942.0	1.01M	1.18	1.18
1st test						
1 hour						
10 hours						
2 days						
1 week						

C20A-2

gain (k)	100		24		15	
α	6.105		7.535		3.828	
	1	2	1	2	1	2
Non Radiation	109.0	102.5	958.0	902.0	1.265M	1.200M
1st test						
1 hour						
10 hours						
2 days						
1 week						

C20A-4

gain (k)	100 x10^{+6}		24		15	
α	3.4 ohms		759		631	
	1	2	1	2	1	2
Non Radiation	39.0	42.0	190.0	201.0	300.0	325.0
1st test						
1 hour						
10 hours						
2 days						
1 week						

-Unless indicated otherwise k and α are K ohms (x10^{+3} ohms)
-1 or 2 indicates amplifier in A1 position on Figures
-All freqs x10^{3} Hz unless followed by M, M=1x10^{+6} Hz

Composite Amplifier 3dB Max Flat H $3.33 \times 10^{+7}$ Rads

C20A-1

gain (k)	100		24		15	
α	6.105		5.535		3.528	
	1	2	1	2	1	2
Non Radiation	116.0		980.0		1.42M	
1st test	111.0	111.0	900.0	900.0	1.42M	1.42M
1 hour						
10 hours						
2 days						
1 week						

C20A-2

gain (k)	100		24		15	
α	6.105		7.535		3.828	
	1	2	1	2	1	2
Non Radiation	112.0		970.0		1.3M	
1st test	110.0	109.0	982.0	982.0	1.4M	1.4M
1 hour						
10 hours						
2 days						
1 week						

C20A-4

gain (k)	100		24		15	
α	3.4×10^{6} ohms		759		631	
	1	2	1	2	1	2
Non Radiation	38.5		200.0		330.0	
1st test	39.0	39.0	190.0	210.0	300.0	344.0
1 hour						
10 hours						
2 days						
1 week						

-Unless indicated otherwise k and are K ohms ($\times 10^{+3}$ ohms)
-1 or 2 indicates amplifier in A1 position on Figures
-All freqs $\times 10^{3}$ Hz unless followed by M, M=$1 \times 10^{+6}$ Hz

Composite Amplifier 3dB Max Flat I $3.33 \times 10^{+7}$ Rads

C20A-1

gain (k)	100		24		15	
α	6.105		5.535		3.528	
	1	2	1	2	1	2
Non Radiation	113.5		942.0		1.4M	
1st test						
24 hours						
48 hours						
1 week						

C20A-2

gain (k)	100		24		15	
α	6.105		7.535		3.828	
	1	2	1	2	1	2
Non Radiation	108.0		942.0		1.29M	
1st test						
24 hours						
48 hours						
1 week						

C20A-4

gain (k)	100		24		15	
α	3.4×10^{6} ohms		759		631	
	1	2	1	2	1	2
Non Radiation	42.0		200.0		330.0	
1st test						
24 hours						
48 hours						
1 week						

-Unless indicated otherwise k and are K ohms ($\times 10^{+3}$ ohms)
-1 or 2 indicates amplifier in A1 position on diagrams.
-All freqs $\times 10^{3}$ Hz unless followed by M, M=$1 \times 10^{+6}$ Hz.

FIVE $5 \times 10^{+4}$ Rads

Slew Rates volts/microseconds

	5A	5B
Non Radiation	7.8	7.5
Test 1	0.68	0.65
24 hours		
48 hours		
1 week		

Single Amplifier 3dB Points

all freqs $\times 10^{3}$

	5A			5B		
gain (k)	100	24	15	100	24	15
Non Radiation	5.5	23.0	35.0	9.6	40.5	63.8
Test 1	5.65	20.5	35.5	9.82	40.5	64.2
24 hours						
48 hours						
1 week						

6 $1 \times 10^{+5}$ Rads

Slew Rates volts/microseconds

	6A	6B
Non Radiation	9.4	9.8
Test 1	0.9	0.95
1 hour		
10 hours		
2 days		
1 week		

Single Amplifier 3dB Frequencies

all frequencies $\times 10^{+3}$ Hz

	6A			6B		
Gain (k)	100	24	15	100	24	15
Non Radiation	12.75	55.0	87.5	13.5	60.0	93.0
Test 1	12.75	55.0	87.5	13.5	60.0	93.0
1 hour						
10 hours						
2 days						
1 week						

8 $5 \times 10^{+5}$ Rads

Slew Rates volts/microseconds

	8A	8B
Non Radiation	6.4	6.6
Test 1	0.64	0.65
1 hour		
10 hours		
2 days		
1 week		

Single Amplifier 3dB Frequencies

all frequencies $\times 10^{+3}$ Hz

	8A			8B		
Gain (k)	100	24	15	100	24	15
Non Radiation	9.30	39.50	62.0	9.65	42.0	66.5
Test 1	9.30	39.00	62.0	9.75	41.5	65.0
1 hour						
10 hours						
2 days						
1 week						

$1x10^{+6}$ Rads

Slew Rates volts/microseconds

	10A	10B
Non Radiation	8.2	8.2
Test 1	0.74	0.73
1 hour		
10 hours		
2 days		
1 week		

Single Amplifier 3dB Frequencies

all frequencies $x10^{+3}$ Hz

	10A			10B		
Gain (k)	100	24	15	100	24	15
Non Radiation	11.3	49.5	77.0	11.6	51.8	81.0
Test 1	10.7	45.0	72.2	11.2	48.0	75.8
1 hour						
10 hours						
2 days						
1 week						

14 $5 \times 10^{+6}$ Rads

Slew Rates volts/microseconds

	14A	14B
Non Radiation	3.5	4.2
Test 1	3.4	3.3
24 hours	0.0	3.2
48 hours	3.7	3.2
1 week	2.6	3.4

Single Amplifier 3dB Points

all freqs $\times 10^{3}$

	14A			14B		
gain (k)	100	24	15	100	24	15
Non Radiation	5.8	23.0	36.5	6.78	27.5	43.5
Test 1	0.0	0.0	0.0	20.0	65.0	105.0
24 hours	0.0	0.0	0.0	37.5	195.0	330.0
48 hours	0.0	73.0	115.0	34.5	175.0	290.0
1 week	0.0	75.0	119.0	34.5	170.0	280.0

15 $5 \times 10^{+6}$ Rads

Slew Rates volts/microseconds

	15A	15B
Non Radiation	6.2	5.9
Test 1	3.4	0.0
24 hours	3.4	0.0
48 hours	3.2	2.8
1 week	3.0	2.9

Single Amplifier 3dB Points

all freqs $\times 10^{3}$

	15A			15B		
gain (k)	100	24	15	100	24	15
Non Radiation	9.7	41.0	65.0	9.1	38.0	60.0
Test 1	19.5	59.5	91.0	0.0	0.0	0.0
24 hours						
48 hours	19.5	96.2	180.0	0.0	96.0	190.0
1 week	21.0	92.0	165.0	0.0	93.0	175.0

Composite Amplifier 3dB Max Flat Five $5x10^{+4}$ Rads

C20A-1

gain (k)	100		24		15	
α	6.105		5.535		3.528	
	1	2	1	2	1	2
Non Radiation	70.0		180.0		200.0	
1st test						
24 hours						
28 hours						
1 week						

C20A-2

gain (k)	100		24		15	
α	6.105		7.535		3.828	
	1	2	1	2	1	2
Non Radiation	45.5		106.0		114.5	
1st test						
24 hours						
48 hours						
1 week						

C20A-4

gain (k)	100		24		15	
α	3.4 $x10^{6}$ ohms		759		631	
	1	2	1	2	1	2
Non Radiation	9.85		42.0		66.5	
1st test						
24 hours						
48 hours						
1 week						

-Unless indicated otherwise k and are K ohms ($x10^{+3}$ ohms)
-1 or 2 indicates amplifier in A1 position on diagrams.
-All freqs $x10^{3}$ Hz unless followed by M, M=$1x10^{+6}$ Hz.

Composite Amplifier 3dB Max Flat Frequencies 6 $1x10^{+5}$ Rads

C20A-1

gain (k)	100		24		15	
α	6.105		5.535		3.528	
	1	2	1	2	1	2
Non Radiation	83.0		285.0		320.0	
1st test						
1 hour						
10 hours						
2 days						
1 week						

C20A-2

gain (k)	100		24		15	
α	6.105		7.535		3.828	
	1	2	1	2	1	2
Non Radiation	101.0		310.0		350.0	
1st test						
1 hour						
10 hours						
2 days						
1 week						

C20A-4

gain (k)	100		24		15	
α	3.4 $x10^{6}$ ohms		759		631	
	1	2	1	2	1	2
Non Radiation	15.8		64.0		110.0	
1st test						
1 hour						
10 hours						
2 days						
1 week						

-Unless indicated otherwise k and are K ohms ($x10^{+3}$ ohms)
-1 or 2 indicates amplifier in A1 position on Figures
-All freqs $x10^{3}$ Hz unless followed by M, M=$1x10^{+6}$ Hz

Composite Amplifier 3dB Max Flat Frequencies 8.5x10^{+5} Rads

C20A-1

gain (k)	100		24		15	
α	6.105		5.535		3.528	
	1	2	1	2	1	2
Non Radiation	67.0		190.0		220.0	
1st test						
1 hour						
10 hours						
2 days						
1 week						

C20A-2

gain (k)	100		24		15	
α	6.105		7.535		3.828	
	1	2	1	2	1	2
Non Radiation	83.0		200.0		238.0	
1st test						
1 hour						
10 hours						
2 days						
1 week						

C20A-4

gain (k)	100		24		15	
α	3.4 x10^{6} ohms		759		631	
	1	2	1	2	1	2
Non Radiation	10.5		44.0		70.0	
1st test						
1 hour						
10 hours						
2 days						
1 week						

-Unless indicated otherwise k and are K ohms (x10^{+3} ohms)
-1 or 2 indicates amplifier in A1 position on Figures
-All freqs x10^{3} Hz unless followed by M, M=1x10^{+6} Hz

Composite Amplifier 3dB Max Flat 10 $1x10^{+6}$ Rads

C20A-1

gain (k)	100		24		15	
α	6.105		5.535		3.528	
	1	2	1	2	1	2
Non Radiation	76.0		240.0		270.0	
1st test	76.0		225.0		252.0	
24 hours						
28 hours						
1 week						

C20A-2

gain (k)	100		24		15	
α	6.105		7.535		3.828	
	1	2	1	2	1	2
Non Radiation	96.0		265.0		300.0	
1st test	86.5		242.0		278.0	
24 hours						
48 hours						
1 week						

C20A-4

gain (k)	100		24		15	
α	3.4 $x10^{6}$ ohms		759		631	
	1	2	1	2	1	2
Non Radiation	12.7		55.0		86.5	
1st test	12.02		51.0		81.0	
24 hours						
48 hours						
1 week						

-Unless indicated otherwise k and are K ohms ($x10^{+3}$ ohms)
-1 or 2 indicates amplifier in A1 position on diagrams.
-All freqs $x10^{3}$ Hz unless followed by M, M=$1x10^{+6}$ Hz.

Composite Amplifier 3dB Max Flat 14 $5x10^{+6}$ Rads

C20A-1

gain (k)	100		24		15	
α	6.105		5.535		3.528	
	1	2	1	2	1	2
Non Radiation	49.0		125.0		135.0	
1st test	0.0		0.0		0.0	
24 hours	0.0		0.0		0.0	
48 hours	0.0		740.0		860.0	
1 week	0.0		760.0		780.0	

C20A-2

gain (k)	100		24		15	
α	6.105		7.535		3.828	
	1	2	1	2	1	2
Non Radiation						
1st test	54.2		116.5		130.0	
24 hours	0.0		0.0		0.0	
48 hours	0.0		870.0		965.0	
1 week	0.0		880.0		960.0	

C20A-4

gain (k)	100		24		15	
α	3.4 $x10^{+6}$ ohms		759		631	
	1	2	1	2	1	2
Non Radiation	7.2		28.2		44.2	
1st test	0.0		0.0		0.0	
24 hours	0.0		0.0		0.0	
48 hours	35.0		175.0		290.0	
1 week	34.0		165.0		275.0	

-Unless indicated otherwise k and are K ohms ($x10^{+3}$ ohms)
-1 or 2 indicates amplifier in A1 position on diagrams.
-All freqs $x10^{3}$ Hz unless followed by M, M=$1x10^{+6}$ Hz.

Composite Amplifier 3dB Max Flat 15 $5 \times 10^{+6}$ Rads

C20A-1

gain (k)	100		24		15	
α	6.105		5.535		3.528	
	1	2	1	2	1	2
Non Radiation	61.0		170.0		185.0	
1st test	0.0		0.0		0.0	
24 hours						
48 hours	150.0		510.0		580.0	
1 week	145.0		510.0		580.0	

C20A-2

gain (k)	100		24		15	
α	6.105		7.535		3.828	
	1	2	1	2	1	2
Non Radiation	84.2		195.0		222.0	
1st test	0.0		0.0		0.0	
24 hours						
48 hours	0.0		530.0		0.0	
1 week	222.0		510.0		602.0	

C20A-4

gain (k)	100		24		15	
α	$3.4 \times 10^{+6}$ ohms		759		631	
	1	2	1	2	1	2
Non Radiation	9.62		40.0		64.5	
1st test	0.0		0.0		0.0	
24 hours						
48 hours	0.0		94.0		190.0	
1 week	0.0		90.0		162.0	

-Unless indicated otherwise k and are K ohms ($\times 10^{+3}$ ohms)
-1 or 2 indicates amplifier in A1 position on diagrams.
-All freqs $\times 10^{3}$ Hz unless followed by M, M=$1 \times 10^{+6}$ Hz.

LIST OF REFERENCES

1. Mikhael, Wasfy B. and Michael, Sherif, "A Systematic General Approach for the Generation of Composite OA's for Extended Frequency Operation," Proceedings of the Midwest Symposium on Circuits and System's, Michigan. August 1982.

2. Gariano, P., Generation of an Optimum High Speed High Accuracy Operational Amplifier, Master's Thesis, Naval Postgraduate School, Monterey, California, December 1985.

3. Olesen, H.L., Radiation Effects on Electronic Systems, p. 2, Plenum Press, New York, 1966.

4. Tallon, R.W., et al., "A Comparison of Ionizing Radiation Damage in NOSFETS From Cobalt-60 Gamma Rays, 0.5 to 22 Mev Protons and 1 to 7 MeV Electrons," To be published in IEEE Trans. Nucl. Sci., December 1985.

5. Northrop Research and Technology Center, Report NRTC-75-5R, Radiation Effects on Oxides, Semiconductors, and Devices, by J.R. Srour, et al., May 1975.

6. Srour, J.R., et al., "Leakage Current Phenomena in Irradiated SOS Devices," IEEE Trans. Nucl. Sci., NS-24, No. 6, pp. 2119-2127, December 1977.

7. Cleveland, D.G., "Dose Rate Effects in MOS Microcircuits," IEEE Trans. Nucl. Sci., NS-31, No. 6, pp. 1348-1353, December 1984.

8. Dawes, W.R., "Radiation Effects Hardening Techniques," paper presented at IEEE Nuclear and Space Radiation Effects Conference, Monterey, California, July 1985.

9. Rudie, N.J., Principles and Techniques of Radiation Hardening, Vol. I, Western Periodicals, 1976.

10. Enge, H.A., Introduction to Nuclear Physics, p. 185, Addison-Wesley, 1966.

11. Berger, M.J. and Seltzer, S.M., "Stopping Power and Ranges of Electrons and Positrons," National Bureau of Standards Interim Report 82-2550, 1982.

12. Dienes, G.J. and Vineyard, G.H., Radiation Effects in Solids, Inter-Science Publishers, New Yor, 1957.

13. Ponaris, R.A., Electrons Irradiation of N Channel Silicon on Sapphire Insulated Gate Field Effect Transistors (IGFET), Master's Thesis, Naval Postgraduate School, Monterey, California, December 1985.

14. Air Force Avionics Laboratory, Wright Patterson Air Force Base, Contract F33615-76-C-1205, Study of Define Design Guidelines for Application to Future Development/ Efforts of Radiation Hardened Linear Integrated Circuits, H.J. Hennecke, et al., December 1977.

15. Sour, J.R., et al., Radiation Effects on Semiconductor Materials and Devices, Harry Diamond Laboratories Tech. Report, 171-4, December 1973.

16. Hart, A.R., et al., Hardness Assurance for Long-Term Ionizing Radiation Effects on Bipolar Structures, Mission Research Corporation, Contract No. DNA 001-76-C-0201, March 1978.

17. Antoniou, A., "Realization of Gyrators Using Operational Amplifiers, and Their Use in RC-Active-Network Synthesis," IEEE Proceedings, Vol. 116, No. 11, pp. 1838-1850, November 1969.

18. Davies, A.C., "The Significance of Nullators, Norators and Nullors in Active-Network Theory," Radio Electron. Eng., Vol 34, pp. 259-267, 1967.

19. Tellegen, B.D., "On Nullators and Norators," IEEE Trans. on Circuit Theory, Vol. Ct-13, pp. 466-469, 1966.

20. Mikhael, Wasfy B. and Michael, Sherif, "Actively Compensated Composite Operational Amplifiers," Midwest Symposium on Circuits and Systems, Albuquerque, New Mexico, June 1981.

21. Millman, J. and Halkias, C., Integrated Electronics; Analog and Digital Circuits and Systems, p. 386, McGraw-Hill, Inc., 1972.

22. Natarajan, S. and Bhattacharyya, B.B., "Design and Some Applications of Extended Bandwidth Finite Gain Amplifiers," J. Franklin Inst., Vol. 305, No. 6, pp. 320-341, June 1978.

23. Natarajan, S. and Bhattacharyya, B.B., "Design of Actively Compensated Finite Gain Amplifiers for High-Frequency Applications," IEEE Trans. Circuits Syst., Vol CAS-27, pp. 1133-1139, December 1980.

24. Barnett, M.T. and Cunneen, W.J., Design and Performance of the Electron Linear Accelerator at the U.S. Naval Postgraduate School, Master's Thesis, Naval Postgraduate School, Monterey, California, December 1966.

25. O'Reilly, P.J., 30 MeV Electron Radiation Damage to InGaAsP LEDs and InGaAs Photodetectors, Master's Thesis, Naval Postgraduate School, Monterey, California, March 1986.

26. Berard, R.W. and Traverso, T.J., Neutron Form Factors From Elastic Electron-Deuteron Scattering Ratio Experiments at Very Low Momentum Transfers, Master's Thesis, Naval Postgraduate School, Monterey, California, March 1973.

27. Arguello, W.R., The Radiation Effects of High Energy Electrons Upon Thermionic Integrated Circuits, Master's Thesis, Naval Postgraduate School, Monterey, California, March 1985.

28. Anspaugh, B.E. and Downing, R.G., "Solar Cell Radiation Handbook," JPL Publication 82-69, 1982.

29. Michael, S., Composite Operational Amplifiers and Their Applications in Active Networks, Doctor's Dissertation, West Virginia University, Morgantown, West Virginia, 1983.

30. Sedra, A.S. and Smith, K.C., Micro-Electronics, CBS College Publishing, New York, 1982.

INITIAL DISTRIBUTION LIST

		No. Copies
1.	Defense Technical Information Center Cameron Station Alexandria, Virginia 22304-6145	2
2.	Library, Code 0142 Naval Postgraduate School Monterey, California 93943-5002	2
3.	Chairman, Department of Electrical and Computer Engineering, Code 62 Naval Postgraduate School Monterey, California 93943-5000	2
4.	Prof Sherif Michael, Code 62Mi Department of Electrical and Computer Engineering Naval Postgraduate School Monterey, California 93943-5000	4
5.	Prof Rudolf Panholzer, Code 62Pz Department of Electrical and Computer Engineering Naval Postgraduate School Monterey, California 93943-5000	1
6.	Prof F. R. Buskirk, Code 61Bs Department of Physics Naval Postgraduate School Monterey, California 93943-5000	2
7.	Major David M. Lohr, USMC P.O. Box 8674 Naval Postgraduate School Monterey, California 93943-5000	4